JOURNAL OF GEOPHYSICAL RESEARCH, VOL. 113, G01009, doi:10.1029/2007JG000415, 2008

A dynamic model of oceanic sulfur (DMOS) applied to the Sargasso Sea: Simulating the dimethylsulfide (DMS) summer paradox

S. M. Vallina,[1,2] R. Simó,[1] T. R. Anderson,[3] A. Gabric,[4] R. Cropp,[4] and J. M. Pacheco[5]

Received 24 January 2007; revised 24 June 2007; accepted 31 October 2007; published 6 February 2008.

[1] A new one-dimensional model of DMSP/DMS dynamics (DMOS) is developed and applied to the Sargasso Sea in order to explain what drives the observed dimethylsulfide (DMS) summer paradox: a summer DMS concentration maximum concurrent with a minimum in the biomass of phytoplankton, the producers of the DMS precursor dimethylsulfoniopropionate (DMSP). Several mechanisms have been postulated to explain this mismatch: a succession in phytoplankton species composition towards higher relative abundances of DMSP producers in summer; inhibition of bacterial DMS consumption by ultraviolet radiation (UVR); and direct DMS production by phytoplankton due to UVR-induced oxidative stress. None of these hypothetical mechanisms, except for the first one, has been tested with a dynamic model. We have coupled a new sulfur cycle model that incorporates the latest knowledge on DMSP/DMS dynamics to a preexisting nitrogen/carbon-based ecological model that explicitly simulates the microbial-loop. This allows the role of bacteria in DMS production and consumption to be represented and quantified. The main improvements of DMOS with respect to previous DMSP/DMS models are the explicit inclusion of: solar-radiation inhibition of bacterial sulfur uptakes; DMS exudation by phytoplankton caused by solar-radiation-induced stress; and uptake of dissolved DMSP by phytoplankton. We have conducted a series of modeling experiments where some of the DMOS sulfur paths are turned "off" or "on," and the results on chlorophyll-a, bacteria, DMS, and DMSP (particulate and dissolved) concentrations have been compared with climatological data of these same variables. The simulated rate of sulfur cycling processes are also compared with the scarce data available from previous works. All processes seem to play a role in driving DMS seasonality. Among them, however, solar-radiation-induced DMS exudation by phytoplankton stands out as the process without which the model is unable to produce realistic DMS simulations and reproduce the DMS summer paradox.

Citation: Vallina, S. M., R. Simó, T. R. Anderson, A. Gabric, R. Cropp, and J. M. Pacheco (2008), A dynamic model of oceanic sulfur (DMOS) applied to the Sargasso Sea: Simulating the dimethylsulfide (DMS) summer paradox, *J. Geophys. Res.*, *113*, G01009, doi:10.1029/2007JG000415.

1. Introduction

[2] The oceanic sulfur cycle, believed to be an important part of the Earth biogeochemical system because of its potential for climate regulation has received considerable attention in the last two decades. However, owing to the complexity of the cycle, in which the whole microbial food web is involved [*Simó*, 2001], some important features regarding its seasonal dynamics remain largely unexplained. Phytoplankton are the primary producers of dimethylsulfoniopropionate (DMSP), the biochemical precursor of dimethylsulfide (DMS), a volatile compound that is ubiquitous in the global surface ocean. Emission of oceanic DMS to the atmosphere [*Bates et al.*, 1992; *Kettle and Andreae*, 2000] is thought to contribute to non-sea-salt sulfate (nss-SO4) production and cloud condensation nuclei (CCN) formation [*Charlson et al.*, 1987; *Andreae and Crutzen*, 1997; *Vallina et al.*, 2007]. The amount of atmospheric CCN is linked to cloud albedo and therefore to the Earth radiative budget [*Twomey*, 1974; *Albrecht*, 1989; *Kaufman et al.*, 2002]. In this regard, a negative feedback between oceanic DMS

[1]Institut de Ciències del Mar de Barcelona, Consejo Superior de Investigaciones Científicas (ICM - CSIC), Barcelona, Spain.
[2]Now at School of Environmental Sciences, University of East Anglia (ENV - UEA), Norwich, UK.
[3]National Oceanography Center (NOC), Southampton, UK.
[4]Faculty of Environmental Sciences, Griffith University, Nathan, Queensland, Australia.
[5]Departamento de Matemáticas, Facultad de Ciencias del Mar, Universidad de Las Palmas de Gran Canaria (FCM - ULPGC), Islas Canarias, Spain.

0148-0227/08/2007JG000415$09.00

production and Earth albedo has been postulated [*Charlson et al.*, 1987].

[3] Intracellular DMSP (also called particulate DMSP or DMSPp) is released to the water as dissolved DMSP (DMSPd) during phytoplankton cell lysis by natural (non-grazing) mortality, zooplankton grazing and virus attacks [*Groene*, 1995; *Yoch*, 2002; *Steinke et al.*, 2002a]. However, the amount of DMSPp varies among phytoplankton groups [*Keller et al.*, 1989; *Keller and Korjeff-Bellows*, 1996] as well as with the physiological state of the cells within each group [*Keller and Korjeff-Bellows*, 1996; *Stefels*, 2000; *Sunda et al.*, 2002; *Bucciarelli and Sunda*, 2003; *Slezak and Herndl*, 2003]. DMSP may also be exuded by phytoplankton living cells as an overflow of energy [*Groene*, 1995; *Stefels*, 2000]. The conversion of DMSP to DMS is mediated by DMSP-lyase, an enzyme that has been found in DMSP-producing phytoplankton groups as well as in numerous groups of DMSP-consuming bacteria [*Groene*, 1995; *Yoch*, 2002; *Zubkov et al.*, 2002; *Niki et al.*, 2000; *Wolfe et al.*, 2002; *Steinke et al.*, 2002b]. Until recently it was believed that the majority of DMS production was due to zooplankton grazing on phytoplankton and bacterial activity on DMSPd [*Levasseur et al.*, 1996; *Dacey et al.*, 1998; *González et al.*, 1999]. However, recent studies suggest that the role of phytoplankton DMS production has been overlooked [*Simó and Pedrós-Alió*, 1999; *Niki et al.*, 2000; *Wolfe et al.*, 2002; *Sunda et al.*, 2002; *Toole and Siegel*, 2004; *Toole et al.*, 2006]. Under conditions of high UV radiation stress or severe nutrient limitation it seems that phytoplankton may be responsible of an important fraction of the total DMS production [*Stefels and van Leeuwe*, 1998; *Wolfe et al.*, 2002; *Sunda et al.*, 2002]. Most groups of oceanic bacteria are able to undertake DMSPd consumption (from which only a small fraction is cleaved to DMS plus acrylate, the rest being demethylated to other forms of sulfur [*Groene*, 1995; *Yoch*, 2002; *Kiene and Linn*, 2000]). DMS is consumed as a carbon source mostly by some methylotrophic bacteria [*Kiene and Bates*, 1990; *Kiene*, 1992, 1993; *Bates et al.*, 1994; *Wolfe et al.*, 1999; *Simó et al.*, 2000; *Yoch*, 2002; *Zubkov et al.*, 2004; *Vila-Costa et al.*, 2006a] or converted to dimethylsulfoxide (DMSO) with energy gain by unknown bacteria [*Vila-Costa et al.*, 2006a; *del Valle et al.*, 2007]. The other major sinks of DMS are photolysis by UV (a process mediated by photosynthesizer substances) [*Brimblecombe and Shooter*, 1986; *Brugger et al.*, 1998; *Toole et al.*, 2003; *Kieber et al.*, 1996] and emission to the atmosphere [*Kettle and Andreae*, 2000]. Also, it has been recently discovered that non DMSP-producing phytoplankton are also able to take up DMSPd, potentially reducing the amount of DMSPd available for bacteria degradation and its conversion to DMS [*Vila-Costa et al.*, 2006b].

[4] Both DMSP and DMS are an integral part of the dissolved organic matter (DOM) pool. The oceanic cycles of DOM and organic sulfur are therefore thought to be tightly coupled [*Vézina*, 2004]. DMSPd appears to be the main source of sulfur (S) for bacteria [*Kiene et al.*, 1999; *Kiene and Linn*, 2000; *Yoch*, 2002; *Zubkov et al.*, 2001, 2002], although it is also a source of carbon (C) [*Yoch et al.*, 1997; *Zubkov et al.*, 2001; *Yoch*, 2002]. On the other hand, DMS is mainly a source of carbon and energy, sulfate and DMSO being the primary fate of sulfur from bacterial consumption of DMS [*Vila-Costa et al.*, 2006a; *del Valle et al.*, 2007]. DMS dynamics are therefore regulated by a complex interplay of biotic and abiotic processes where phytoplankton, zooplankton and bacteria are believed to have a prominent role.

[5] With the aim at gaining a better understanding on the processes governing the oceanic sulfur cycle, several dynamic (i.e. mechanistic) models of DMSP/DMS have been developed in the last decade or so [*Gabric et al.*, 1993; *Lawrence*, 1993; *van den Berg et al.*, 1996; *Laroche et al.*, 1999; *Jodwalis et al.*, 2000; *Archer et al.*, 2002; *Lefevre et al.*, 2002; *Chu et al.*, 2004]. These models usually consist of two submodels: a nitrogen based one (N-cycle) characterizing the ecosystem, and a sulfur based one (S-cycle) of the DMSP/DMS dynamics [*Vézina*, 2004]. These two submodels are coupled but without feedbacks between them: the N-cycle affects the S-cycle, but not viceversa [*Vézina*, 2004]. Most of these models do not, however, include a characterization of the microbial loop, that is, an explicit representation of bacteria, bacterivory, and the DOM cycle. This is due to the fact that the first ecosystem models did not give sufficient relevance to the microbial loop.

[6] However, in recent years, bacteria and DOM dynamics have gained relative importance in ecosystem models and it has been shown that their inclusion is fundamental in order to obtain realistic simulations of the seasonal cycles of the model state variables [*Spitz et al.*, 2001]. In the Sargasso Sea, for example, most of the carbon cycling is through the microbial loop [*Steinberg et al.*, 2001, and references therein]. The DMSP/DMS model of *Archer et al.* [2002] (which is based on the ERSEM ecosystem model [*Baretta et al.*, 1995]) is the only ecosystem model to additionally incorporate bacteria and DOM dynamics. Although the model of *Gabric et al.* [1993] incorporated bacteria as part of the N-cycle, bacteria were not explicitly represented in the S-cycle. Rather, bacterial effects on DMSP and DMS concentrations were parameterized as constant rates, independently of their evolution in the N-cycle. This is probably due to the fact that the N-cycle of Gabric's model (which is based on *Moloney et al.* [1986]) does not include DOM dynamics, such that predicted bacteria display "catastrophic behavior", being close to zero for much of the time [*Cropp*, 2002; *Cropp et al.*, 2004]. Variations in bacterial sulfur demand have been suggested to affect DMS production, so that if DMSPd is in excess of bacterial requirements for sulfur, a larger proportion of the DMSPd taken up could be converted to DMS [*Kiene et al.*, 1999]. Therefore, *Cropp* [2002] recommends that a priority for the next generation of DMSP/DMS models is the inclusion of a realistic microbial loop. Similar conclusions were reported by other authors [*Lefevre et al.*, 2002; *Le Clainche et al.*, 2004; *Vézina*, 2004].

[7] Another significant problem with most of the current DMSP/DMS models is the difficulty of decoupling DMS dynamics from that of phytoplankton. It has been observed that DMS peaks in summer at tropical, subtropical and low temperate latitudes, a time when chlorophyll-a (CHL, a common proxy for phytoplankton biomass) is at its annual minimum [*Simó and Pedrós-Alió*, 1999; *Uher et al.*, 2000; *Toole and Siegel*, 2004; *Vallina et al.*, 2006; *Vila-Costa et al.*, 2008]. This finding has been dubbed the "DMS summer paradox" [*Simó and Pedrós-Alió*, 1999]. Several mechanisms have been proposed to explain it, such as a succession

in phytoplankton species composition towards high DMSPp producers, inhibition of bacterial DMS consumption by high UV, and a higher (direct) production of DMS from phytoplankton cells due to UV stress [*Simó and Pedrós-Alió*, 1999; *Sunda et al.*, 2002; *Toole and Siegel*, 2004]. Most of these potential explanations have not as yet been tested in models. The model of *Lefevre et al.* [2002] and the parameterization used by *Gabric et al.* [2005] are the sole examples of including a variable sulfur to nitrogen (S:N) phytoplankton internal quota as a function of light in order to account for a shift in species composition and/or a change in phytoplankton physiological state. This allowed a higher degree of decoupling between DMS and CHL in these models. It was, however, shown by *Le Clainche et al.* [2004] for the Sargasso Sea (using the same model as *Lefevre et al.* [2002] but coupled to a dynamic turbulent scheme) that the seasonality of modeled DMS was lower than that of DMS observations and the summer maximum was underestimated.

[8] In this work we present a Dynamic Model of Oceanic Sulfur (DMOS) which is based on a modified version of the ecosystem model (N/C-cycles) developed by *Anderson and Pondaven* [2003] (hereafter AP'03). It has an explicit representation of bacteria and DOM dynamics, and is adapted for the Sargasso Sea using data collected during the Bermuda Atlantic Time-series Study (BATS) [*Steinberg et al.*, 2001]. We have coupled a new S-cycle to it that incorporates the latest knowledge of DMSP/DMS dynamics. Model complexity was progressively increased in order to test several of the hypotheses generally used to explain the DMS summer paradox. The performance of the model in simulating annual cycles of concentrations, fluxes and turnover rates of the sulfur variables is analyzed.

2. Data and Methodology

2.1. Sargasso Sea Data

[9] The Sargasso Sea is located in the subtropical West North Atlantic and represents an oligotrophic open ocean region where the DMS summer paradox is readily observable [*Dacey et al.*, 1998; *Toole and Siegel*, 2004]. Phytoplankton seasonality is regulated by physical processes which drive the deep nutrient entrainment in the upper layers during winter and spring, followed by nutrient depletion in summer due to a strong stratification of the water column [*Goericke*, 1998; *DuRand et al.*, 2001; *Steinberg et al.*, 2001]. The dominant phytoplankton groups are prokariotic picophytoplankton (Prochlorococcus and Synechococcus) and eukariotic phytoplankton (Prymnesiophytes, Pelagophytes) [*Goericke*, 1998; *DuRand et al.*, 2001; *Steinberg et al.*, 2001]. Diatoms are not a dominant group, although rare episodic blooms have been observed [*Steinberg et al.*, 2001]. Dinoflagellates are also represented as a low percentage of the phytoplankton community [*Goericke*, 1998; *Steinberg et al.*, 2001]. The mixed layer depth (MLD) has a marked seasonal cycle with values from ≈200 m to less than 10 m in summer [*Steinberg et al.*, 2001; *Spitz et al.*, 2001] and the sea surface temperature (SST) varies from ≈20° in winter to ≈28° in summer [*Steinberg et al.*, 2001].

[10] During the Bermuda Atlantic Time-series Study, station BATS (31.75°N, 64.17°W) was sampled for vertically resolved profiles of CHL and bacteria (along with many other physical and biological variables) approximately monthly from 1989. Data are available at the BATS database (http://bats.bbsr.edu/). Hydrostation-S (32.17°N, 64.50°W) has been sampled for vertically resolved profiles of DMSPp, DMSPd and DMS approximately biweekly from 1992 to 1994 [*Dacey et al.*, 1998; *Toole and Siegel*, 2004]. Using these depth resolved time series we have constructed two-dimensional (2-D; time and depth) climatologies of CHL and bacteria (more than 10 years of data, from 1989 to 2000) as well as DMSPp, DMSPd and DMS (three years of data, from 1992 to 1994). The methodology used for building the climatology was as follows. All measured profiles were merged by month. Then, for each month, a 6th degree polynomial regression was used to fit the cloud of data, obtaining a single depth-resolved profile per month. Finally the resulting monthly profiles were interpolated in time, generating 2-D (time, depth) plots with a resolution of 1 day × 1 m. To be consistent, model results were also interpolated in depth and averaged in time to obtain the same 1 day × 1 m resolution (see section 3. Results and Discussion). DMSPd did not display a clear seasonal pattern over the sampling period [*Dacey et al.*, 1998] and therefore the obtained climatology has to be viewed with some caution. On the other hand, DMSPp and DMS showed a much clearer seasonal cycle.

2.2. Model Description

[11] The AP'03 ecosystem model includes a detailed characterization of the microbial loop. It incorporates a complex description of the DOM cycle and explicitly includes heterotrophic bacteria as a state variable. The treatment of DOM includes dual currencies, nitrogen (DON) and carbon (DOC). Since DMSP and DMS are part of the DOM, and therefore they share many of their processes (such as bacterial uptake and degradation), a DMSP/DMS model including a detailed microbial loop is fundamental [*Vézina*, 2004]. We thus coupled our S-cycle model to the AP'03 N/C-cycles, calling this coupled ecosystem-DMSP/DMS model "DMOS" (Dynamic Model of Oceanic Sulfur). The new S-cycle model contains important improvements like the explicit representation of bacterial activity in the sulfur cycle (including for the first time UV inhibition of bacterial sulfur uptake), a time-varying DMS exudation term from phytoplankton (due to UV stress) as well as an uptake of DMSPd for phytoplankton. In a manner similar to *Archer et al.*, 2002, we include nonlinear kinetics for sulfur uptake (other models use linear relationships [*Vézina*, 2004]).

[12] One of the advantages of including bacteria explicitly in DMSP/DMS models is that it is then possible to evaluate the relative contributions of phytoplankton and bacteria to the DMS production, this being one of the important unanswered questions concerning the biogeochemistry of DMS [*Yoch*, 2002]. Further, the DMS-yield of the whole food web (total DMS production/total DMSP consumption), which is a very sensitive parameter in DMSP/DMS models [*Lefevre et al.*, 2002; *Vézina*, 2004; *Le Clainche et al.*, 2004; *Cropp et al.*, 2004] is not prescribed as an a-priori parameter: it is now an output of the model (see section 3. Results and Discussion). The full set of DMOS equations is described in Appendix A. Model

Table 1. List of DMOS Parameters

Parameter	Symbol	Value	Unit	Source
Phyto. max. specific growth rate	$\mu_P^{\max}$	3.7	$[d^{-1}]$	*Spitz et al.* [2001]
Phyto. saturating irradiance	I_s	60	[W m^{-2}]	*Cropp et al.* [2004]
Phyto. half-sat. for NO_3 = uptake	k_P^N	0.15	[mmolN m^{-3}]	*Anderson and Pondaven* [2003]
Phyto. half-sat. for NH_4^+ uptake	k_P^A	0.05	[mmolN m^{-3}]	*Anderson and Pondaven* [2003]
Phyto. NH_4^+ inhibition parameter	ψ	1.5	[$mmolN^{-1}$]	*Anderson and Pondaven* [2003]
Phyto. leakage fraction	γ_1	0.05	[*adim*]	*Anderson and Pondaven* [2003]
Phyto. DOC exudation parameter	γ_2	0.34	[*adim*]	*Anderson and Pondaven* [2003]
Phyto. specific mortality rate	m_P	0.045	$[d^{-1}]$	*Anderson and Pondaven* [2003]
Phyto. mortality losses to DOM	ε	0.34	[*adim*]	*Anderson and Pondaven* [2003]
Phyto. sinking rate	$\lvert\vec{w_p}\rvert$	0.05	[$m\ d^{-1}$]	This study
Phyto. C:N ratio	$\theta_{Pc:n}$	6.625	[mmolC $mmolN^{-1}$]	*Anderson and Pondaven* [2003]
Phyto. $CaCO_3$:C ratio	θ_{Ca}	0.10	[mmolC $mmolC^{-1}$]	*Anderson and Pondaven* [2003]
Phyto. max. CHL:C ratio	θ_{chl}^m	0.041	[mgCHL mgC−1]	*Spitz et al.* [2001]
Phyto. initial slope of P-I curve	α_{chl}	1.0	[mgC $mgCHL^{-1}$ $(W\ m^{-2})^{-1}\ d^{-1}$]	*Spitz et al.* [2001]
Phyto. molecular weight of Carbon	C_{mw}	12	[mgC $mmolC^{-1}$]	*Spitz et al.* [2001]
Phyto. min. S:N internal quota	$\theta_{Ps:n}^{\min}$	0.044	[mmolS $mmolN^{-1}$]	*Lefevre et al.* [2002]
Phyto. max. S:N internal quota	$\theta_{Ps:n}^{\max}$	0.220	[mmolS $mmolN^{-1}$]	*Lefevre et al.* [2002]
Phyto. max. DMS specific exudation rate	$\gamma_s^{\max}$	0.25	$[d^{-1}]$	This study
Phyto. fraction of DMSPd consumers	α_P	0.1	[*adim*]	This study
Phyto. free DMSP-lyase activity	f	0.01	$[d^{-1}]$	This study
Zoo. max. specific ingestion rate	g	3.2	$[d^{-1}]$	This study
Zoo. N assim. efficiency	β_n	0.75	[*adim*]	*Anderson and Pondaven* [2003]
Zoo. C assim. efficiency	β_c	0.65	[*adim*]	*Anderson and Pondaven* [2003]
Zoo. C net growth efficiency	ω_Z	0.8	[*adim*]	*Anderson and Pondaven* [2003]
Zoo. half-sat. const. for N ingestion	k_g	0.75	[mmolN m^{-3}]	*Anderson and Pondaven* [2003]
Zoo. grazing preference upon Phyto.	p_P	1/3	[*adim*]	*Anderson and Pondaven* [2003]
Zoo. grazing preference upon Bact.	p_B	1/3	[*adim*]	*Anderson and Pondaven* [2003]
Zoo. grazing preference upon Det.	p_D	1/3	[*adim*]	*Anderson and Pondaven* [2003]
Zoo. C:N ratio	$\theta_{Zc:n}$	5.5	[mmolC $mmolN^{-1}$]	*Anderson and Pondaven* [2003]
Zoo. messy feeding losses to DOM	ϕ	0.23	[*adim*]	*Anderson and Pondaven* [2003]
Zoo. max. specific mortality rate	m_Z	0.3	$[d^{-1}]$	*Anderson and Pondaven* [2003]
Zoo. half-sat. const. for mortality	k_Z	0.2	[mmolN m^{-3}]	*Anderson and Pondaven* [2003]
Zoo. mortality fraction going to DOM	Ω_{dom}	0.38	[*adim*]	*Anderson and Pondaven* [2003]
Zoo. mortality fraction going to NH_4^+	Ω_A	0.33	[*adim*]	*Anderson and Pondaven* [2003]
Zoo. mortality fraction going to Detritus-N	Ω_{Dn}	0.29	[*adim*]	*Anderson and Pondaven* [2003]
Zoo. mortality fraction going to Detritus-C	Ω_{Dc}	0.46	[*adim*]	*Anderson and Pondaven* [2003]
Zoo. mortality fraction going DIC	Ω_{DIC}	0.16	[*adim*]	*Anderson and Pondaven* [2003]
Zoo. DMSPp ingestion: fraction converted to DMSPd	α_1	0.7	[*adim*]	*Simó* [2004]
Bact. max. Lc/NH_4^+ and sulfur uptake	$\mu_B^{\max}$	13.3	$[d^{-1}]$	*Anderson and Pondaven* [2003]
Bact. max. Sc hydrolysis	μ_{Sc}	4	$[d^{-1}]$	*Anderson and Pondaven* [2003]
Bact. half-sat. const. for NH_4^+ uptake	k_A	0.5	[mmolN m^{-3}]	*Anderson and Pondaven* [2003]
Bact. half-sat. const. for Lc uptake	k_{Lc}	25	[mmolC m^{-3}]	*Anderson and Pondaven* [2003]
Bact. half-sat. const. for Sc hydrolysis	k_{Sc}	417	[mmolC m^{-3}]	*Anderson and Pondaven* [2003]
Bact. max. inhibition by UV of nutrient uptake	$\phi_{inhib}^{\max}$	0.75	[*adim*]	This study
Bact. specific nitrification rate	v	0.03	$[d^{-1}]$	*Anderson and Pondaven* [2003]
Bact. C gross growth efficiency	ω_B	0.17	[*adim*]	*Anderson and Pondaven* [2003]
Bact. specific mortality rate	m_B	0.04	$[d^{-1}]$	*Anderson and Pondaven* [2003]
Bact. C:N ratio	$\theta_{Bc:n}$	5.1	[mmolC $mmolN^{-1}$]	*Anderson and Pondaven* [2003]
Bact. S:C ratio	$\theta_{Bs:c}$	1/250	[mmolS $mmolC^{-1}$]	*del Valle et al.* [2007]
Bact. fraction of DMS consumers	α_B	0.20	[*adim*]	This study
Bact. half-sat. const. for DMSPd uptake	k_{DMSPd}	0.01	[mmolS m^{-3}]	This study
Bact. half-sat. const. for DMS uptake	k_{DMS}	0.01	[mmolS m^{-3}]	This study
Bact. DMSPd excess uptake: fraction converted to DMS	α_2	0.1	[*adim*]	*Kiene and Linn* [2000]
Labile fraction of DOM produced	δ_1	0.7	[*adim*]	*Anderson and Pondaven* [2003]
Labile fraction of Phyto. extra-DOC exudation	δ_2	0.4	[*adim*]	*Anderson and Pondaven* [2003]
Detrital-N breakdown rate	m_{Dn}	0.055	$[d^{-1}]$	*Anderson and Pondaven* [2003]
Detrital-C breakdown rate	m_{Dc}	0.04	$[d^{-1}]$	*Anderson and Pondaven* [2003]
Detrital-$CaCO_3$ dissolution rate	m_{Dh}	0.05	$[d^{-1}]$	*Anderson and Pondaven* [2003]
Detrital sinking rate	$\lvert\vec{w_{Di}}\rvert$	0.05	[m d^{-1}]	This study
Irradiance max.	$I_{\max}$	150	[W m^{-2}]	This study
Irradiance min.	$I_{\min}$	45	[W m^{-2}]	This study
Irradiance threshold	I^*	25	[W m^{-2}]	*Lefevre et al.* [2002]
Irradiance attenuation due to water	k_w	0.04	$[m^{-1}]$	*Popova et al.* [2002]
Irradiance attenuation due to Phyto. self-sheding	k_p	0.03	[m^2 $mmolN^{-1}$]	*Popova et al.* [2002]
Max. specific DMS photolysis rate	$k_{photo}^{\max}$	0.15	$[d^{-1}]$	*Bailey et al.* [2008]
Max. turbulent diffusion	$kz_{\max}$	250	[$m^2\ d^{-1}$]	*Cropp et al.* [2004]
Min. turbulent diffusion	$kz_{\min}$	1	[m^2 d^{-1}]	*Cropp et al.* [2004]
Max. sea temperature (changes each day)	$st_{\max}$	SST	[°C]	This study
Min. sea temperature	$st_{\min}$	19	[°C]	This study
Steepness of the pycnocline	r	−20	[*adim*]	*Cropp et al.* [2004]

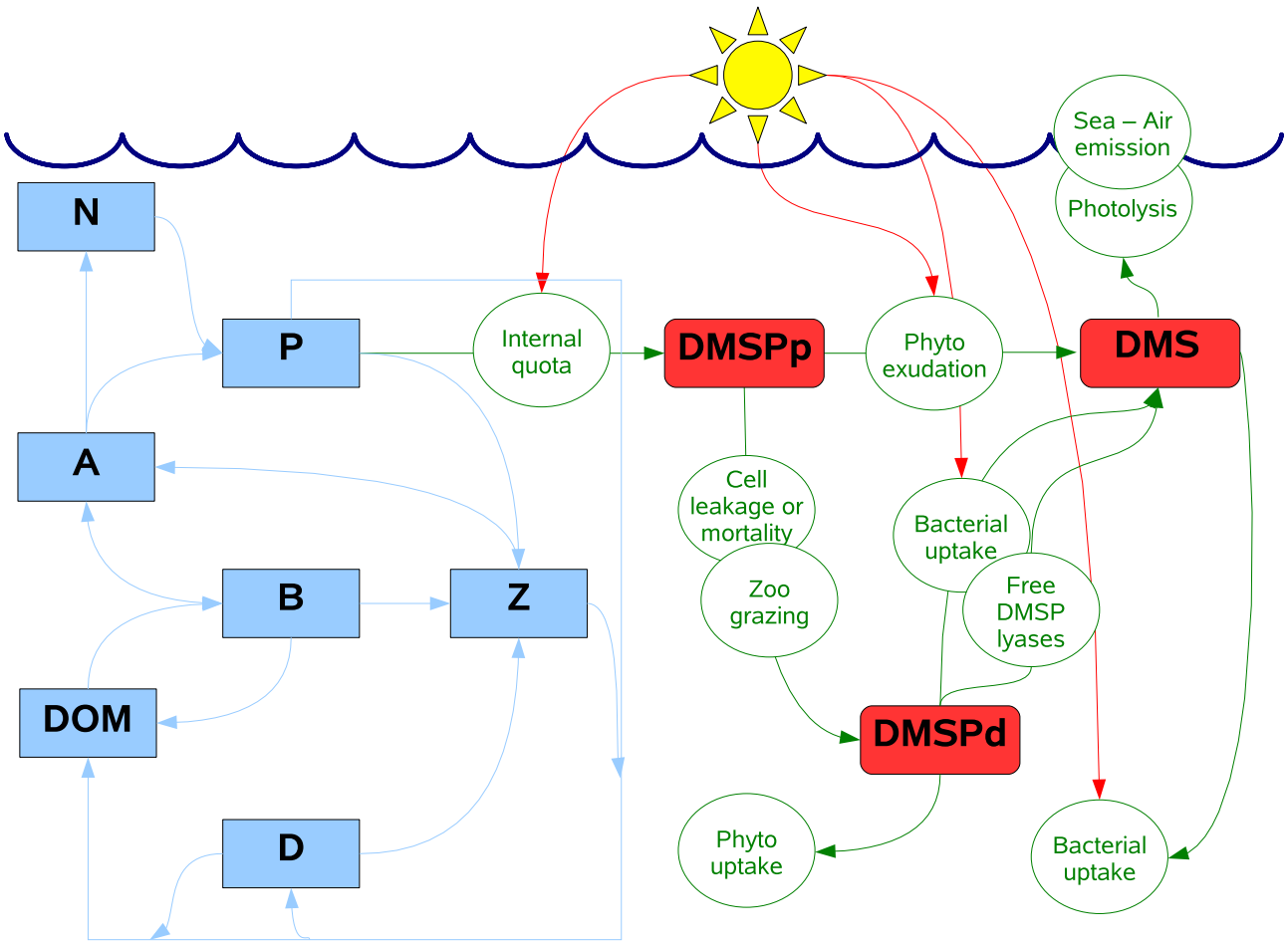

Figure 1. Schematic diagram of DMOS model. (left) Ecosystem submodel: (N/C-cycles; mmol m^{-3}) A, ammonium; N, nitrates; P, phytoplankton; B, bacteria; Z, zooplankton; DOM, dissolved organic matter (can be either nitrogen based or carbon based, and labile or semilabile); D, detritus (can be either nitrogen based or carbon based). Note that the modeled cycling of dissolved organic matter and detritus has been purposely simplified in this diagram as a generic DOM and D pools for clarity; a more detailed scheme of the ecosystem submodel can be found in the work of *Anderson and Pondaven* [2003]. (right) DMSP/DMS submodel (S-cycle; mmol m^{-3}): DMSPp, particulated dimethylsulfoniopropionate; DMSPd, dissolved dimethylsulfoniopropionate; DMS, dimethylsulfide. The red lines coming from the Sun refer to the S-cycle processes directly affected by solar radiation in DMOS model that has been tested by the five modeling experiments performed.

parameters are listed in Table 1. An schematic diagram of DMOS model is shown in Figure 1.

2.3. N/C-Cycles

[13] The model contains single state variables for phytoplankton (equation (A1)), zooplankton (equation (A2)) and heterotrophic bacteria (equation (A3)), two nutrient pools (nitrate (equation (A4)) and ammonium (equation (A5))), labile and semilabile DON and DOC (equations (A6 –A9)), detritus (equations (A10–A12)), dissolved inorganic carbon (DIC, equation (A13)) and alkalinity (equation (A14)). CHL (equation (A15)) is calculated for phytoplankton N at each time step based upon *Geider et al.* [1997] as in *Spitz et al.* [2001], permitting comparison with field data. Phytoplankton primary production (equation (A19)) is controlled by light (equation (A22)) [*Walsh et al.*, 2001] and temperature (equation (A21)) [*Eppley*, 1972], affecting the specific growth rate (equation (A20)), as well as by nutrient availability (equation (A25)) [*Spitz et al.*, 2001]. Phytoplankton losses are due to zooplankton grazing (equation (A29)), natural mortality (equation (A55)) and vertical sinking (equation (A80)). Zooplankton graze upon phytoplankton, bacteria and soft detritus (equations (A29–A32)). Zooplankton production (equation (A37) or equation (A39)), ammonium excretion (equation (A38) or equation (A40)), and respiration (equation (A41)) are calculated according to a stoichiometric model [*Anderson and Hessen*, 1995; *Anderson and Pondaven*, 2003]. Zooplankton mortality is assumed to occur in the form of a quadratic Michaelis-Menten equation (equation (A56)). This is a classical way of parameterizing both natural mortality and grazing by higher predators (which are not explicitly modeled). Bacteria production, excretion and respiration (equations (A47–

A52)) are calculated from elemental stoichiometry [*Anderson*, 1992; *Anderson and Williams*, 1998; *Anderson and Pondaven*, 2003]. Labile DOC and DON are the primary growth substrates, with ammonium supplementing DON when the ratio DOC/DON (C:N ratio of DOM) is high. Uptake of labile DOC and DON and the maximum potential uptake of ammonium are described in equations (A43)–(A45). Bacteria either take up or regenerate ammonium at any one time depending on the availability of DOC and DON (equation (A47)), an upper limit of ammonium uptake being given by equation (A44). The fraction of DOC taken up not used for balanced (C:N) growth is respired (equation (A49) or equation (A52)). Bacteria loss terms are zooplankton grazing (equation (A30)) and natural mortality (equation (A57)).

[14] The main sink for nutrients is phytoplankton uptake (equation (A19)), ammonium also being lost to the nitrate pool via nitrification at constant rate (see second term on equation (A5)). The DOM pools are produced by phytoplankton leakage, excretion and exudation, zooplankton messy feeding, phytoplankton and bacterial natural mortality, and noncarbonate detrital breakdown (equations (A58–A59)). The semilabile DOM pool is converted to labile DOM due to the action of exoenzymes by bacterial (equations (A53–A54)). Phytoplankton exudation of DOC is directly proportional to primary production (see equation (A28)). Noncarbonate (or soft) detritus (equations (A10–A11)) arises from zooplankton egestion as well as phytoplankton and zooplankton mortality, and is lost by zooplankton grazing (equations (A31–A32)), breakdown, and vertical sinking (equation (A80)). The carbonate (or hard) detritus (equation (A12)) originates from the contribution of carbonate-forming (e.g. organisms such as coccolithophores to primary production). This is parameterized assuming a constant $CaCO_3$:C ratio for phytoplankton (see Table 1). The carbonate fraction of total detritus is variable (for soft tissue and carbonate production, and also as additional carbon fixed as DOC), and returned by zooplankton and bacteria respiration as well as zooplankton mortality. Other return pathways, such as breakdown of carbonate detritus (equation (A60)), occur via cycling of DOC. Exchange of CO_2 with the atmosphere can also be estimated (F_{atm} term in equation (A13)) although it is not necessary for our purposes. Parameterization of alkalinity (equation (A14)) is performed according to the stoichiometry described by *Broecker and Peng* [1982].

2.4. S-Cycle

[15] DMSPp (equation (A16)) production by phytoplankton is modeled by using a sulfur/nitrogen (S:N) internal quota ($\theta_{Ps:n}$ parameter, see Table 1). $\theta_{Ps:n}$ is allowed to vary as function of light intensity following *Lefevre et al.* [2002] (equations (A63–A64)). Since the model has only one generic phytoplankton group, this method permits an implicit simulation of a shift in species composition towards high DMSPp producers in summer and/or a shift in phytoplankton physiological state [*Lefevre et al.*, 2002], one of the proposed explanations of the DMS summer paradox. DMSPp is released to the water as DMSPd (equation (A17)) due to phytoplankton leakage and natural mortality as well by zooplankton grazing. It is assumed that 70% of the grazed DMSPp is recovered in the dissolved phase [*Levasseur et al.*, 2004; *Simó*, 2004]. The DMSPd losses are bacterial (equation (A68)) and phytoplankton uptake (equation (A67)) as well as cleavage to DMS by free DMSP-lyases (as in *Archer et al.* [2002]). Bacterial uptake of DMSPd is a well known sink for DMSPd since this compound is a major source of reduced sulfur for apparently most of marine bacteria [*Kiene and Linn*, 2000; *Yoch*, 2002; *Zubkov et al.*, 2002; *Vila et al.*, 2004; *Vila-Costa et al.*, 2007]. A close seasonal correlation between DMSP assimilation by bacteria and bacterial heterotrophic production (measured as leucine incorporation) has been observed recently in a Mediterranean coastal site [*Vila-Costa*, 2006]. We therefore assumed that DMSPd consumption is proportional to the total bacterial community in the model. On the other hand, various phytoplankton take up DMSPd such as diatoms, Synechococcus and Prochlorococcus, these all being low or non DMSP producers [*Vila-Costa et al.*, 2006b; *Malmstrom et al.*, 2004]. With current uncertainties regarding what fraction of total phytoplankton biomass is able to take up DMSPd and at what rates, we considered that this process is carried out by 10% of the phytoplankton (see parameter α_P in Table 1).

[16] In the model, DMS (equation (A18)) production has 3 sources: cleavage from DMSPd by bacteria (equations (A71–A72)) and free DMSP-lyases (3rd term in equation (A18)) as well as direct exudation by phytoplankton (equation (A65)). The total amount of sulfur required by bacteria for balanced (C:S) growth (also called bacterial sulfur demand) is given by equation (A70). If the DMSPd taken up is in excess of bacterial sulfur demand (no S-limitation), a fraction (α_2, see Table 1) of this sulfur excess is cleaved to DMS (equation (A71)), the remainder being converted to other forms of sulfur (e.g. sulfates via the methanethiol pathway) [*Kiene*, 1996; *Kiene and Linn*, 2000; *Kiene et al.*, 2000]. It has been observed experimentally that bacterial production of methanethiol dominates over DMS production [*Kiene*, 1996; *Kiene and Linn*, 2000; *Zubkov et al.*, 2002]. Bacterial DMS-yield rarely goes beyond 10%. Recent works found a range between 2 and 12% (Slezak, personal communication). Similar values were reported by *Kiene and Linn* [2000] and [*Zubkov et al.*, [2002] (6–12%). Therefore α_2 is assumed to be small (10%) [*Kiene and Linn*, 2000; *Niki et al.*, 2000]. On the other hand, if the DMSPd taken up by bacteria is lower than the requirement for balanced (C:S) growth (S-limitation), DMS is not produced (equation (A72)) because sulfur is fixed exclusively into proteins.

[17] Phytoplankton direct exudation of DMS has been assumed to be constant and very small in some models [e.g., *Gabric et al.*, 1993; *Chu et al.*, 2004], with many models not even including it as a process. Recent field research have however suggested that phytoplankton is likely an important source of DMS, mainly under high UV stress [*Toole and Siegel*, 2004; *Toole et al.*, 2006; *Vila-Costa et al.*, 2008]. In support of these findings, the work of *Sunda et al.* [2002] showed increases up to 3500% in the amount of DMS per unit cell volume in phytoplankton cultures exposed to high doses of UV-A. They proposed that DMS acts as an efficient hydroxyl radical scavenger, i.e. as an intracellular antioxidant under conditions of high UV exposure. In the model, therefore, direct exudation of DMS was made

a function of light intensity (first fraction in equation (A66)), although the level of phytoplankton activity is also taken into account (second fraction in equation (A66)).

[18] There is only one biological loss for DMS, namely its uptake by bacteria (equation (A69)). The complete phylogeny of marine DMS-consuming bacteria is not known, but a recent study has shown that the use of DMS as a C source seems mostly restricted to some methylotrophic bacteria [*Vila-Costa et al.*, 2006a], yet DMS consumption as a source of energy by unknown bacteria (conversion to DMSO without use of the C) might be more common [*del Valle et al.*, 2007]. Therefore DMS consumption seems to be not as widespread a process among bacterioplankton as DMSPd utilisation [*Vila-Costa et al.*, 2006a]. Thus, we assumed that only a fraction (20%, see parameter α_B in Table 1) of the generic pool of modeled bacteria acts as a sink for DMS. The other two sinks for DMS in the model are photolysis and emission to the atmosphere. Photolysis is assumed to be solely a function of light intensity (equation (A73)) although in reality it is a process mediated by chromophoric DOM (or CDOM) [*Brimblecombe and Shooter*, 1986; *Brugger et al.*, 1998; *Toole et al.*, 2003], which is not modeled in the current version of DMOS. DMS emission to the atmosphere (equation (A75)) is parameterized with the gas transfer model of *Nightingale et al.* [2000] (equations (A76)–(A78)) using climatological (1992-1994) surface wind speed (U, m s^{-1}) from the NCEP/NCAR Reanalysis Project (provided by the NOAA-CIRES Climate Diagnostics Center). Monthly data were interpolated in time and smoothed to generate daily values.

[19] Regarding the bacterial uptake of nutrients (either labile DON/DOC or NH_4^+) and sulfur (either DMSPd or DMS), the model includes a light inhibition parameter that influences the specific rate of bacterial uptake (equation (A45)). This parameter accounts for the well known effect of UVR upon bacterial heterotrophic activity and bacterial DMSP/DMS consumption [*Herndl et al.*, 1993; *Slezak et al.*, 2001; *Toole et al.*, 2006]. We assume a maximum inhibition of bacterial uptake of 75% (see $\phi_{inhib}^{\max}$ in Table 1) [*Slezak et al.*, 2001; *Toole et al.*, 2006].

2.5. Physical Frame and Forcings

[20] The biogeochemical model is embedded in a one-dimensional (1-D) vertical physical frame. The model therefore neglects horizontal transport processes and takes into account only vertical processes, i.e. advection (equation (A80)) and diffusion (equation (A81)), which are considered the main driving forces of ecosystem dynamics in the upper ocean [*Eigenheer et al.*, 1996; *Denman and Peña*, 1999]. As in the models of *Lefevre et al.* [2002] and *Cropp et al.* [2004], vertical mixing in the current version of DMOS is parameterized using a prescribed turbulent diffusion coefficient (kz, Table 1) following the approach used by *Cropp et al.* [2004]. Coefficient kz is generated using a sigmoid equation (equation (A82)) and climatological MLD data [*Levitus*, 1982]. As a result the maximum diffusion ($kz_{\max}$) occurs in the upper mixed layer (UML) and the minimum diffusion ($kz_{\min}$) occurs below the UML. In between, kz decreases from $kz_{\max}$ to $kz_{\min}$ as dictated by the parameter r (Table 1) which defines the steepness of the pycnocline [*Cropp et al.*, 2004]. The same sigmoid function (equation (A82)) is used to generate the vertical temperature profiles, the only difference being that the maximum value for temperature is the sea surface temperature (SST) which varies seasonally, instead of being constant as for diffusion. SST data for the Sargasso Sea were obtained from a climatology (1971-2000, NOAA-CIRES Climate Diagnostics Center). Monthly data were interpolated in time and smoothed to generate daily values.

[21] Light in the model (I_z, W m^{-2}) is defined as daily averaged photosynthetic available radiation (PAR). Daily values of PAR at the surface (I_0) of the Sargasso Sea were obtained after interpolating in time and smoothing a SeaWiFS climatology (from years 2002 to 2004). Light decays with depth (z, in metres) following an exponential function (equation (A23)) that depends on water and phytoplankton. In the current version of DMOS we wanted to explore if the observed DMS seasonality could be simulated through the inclusion of light-driving processes, with the assumption that UVR is the forcing behind these processes (e.g. bacterial inhibition, phytoplankton stress), yet bacterial inhibition of sulfur uptakes has been also described to occur under PAR [*Slezak et al.*, 2001]. PAR seasonality can be used as a proxy for UVR seasonality, UVR being a constant fraction of PAR. Given that all the parameterizations used to account for UVR-driven processes are based on the term $\frac{I_z}{I_{\max}}$, the constant fraction cancels out and we are just left with a nondimensional term representing UVR that varies between 0 and 1. While UVR attenuates faster in the water column than PAR, the UVR driving processes affecting DMS production may operate at higher depths. It has been described that organisms need some time for recovering after being exposed to high UVR doses [*Toole et al.*, 2006]. Therefore when they escape from the UV zone (i.e. by sinking and/or turbulent diffusion) they may keep a ''memory'' of the stress deeper in the water column. Nevertheless, exploring the use of an explicit wavelength-resolved UVR formulation, with the inclusion of CDOM as a state variable, is desirable and will be object of future research.

[22] The model domain is from 0 to 200 m with a vertical resolution of 2.5 m. Initial conditions (in mmol m^{-3}) are constant profiles for all variables: 0.1 for phytoplankton, zooplankton and bacteria; 2.0 for nitrates; 0.5 for ammonium and labile DON; 24 for labile DOC; 2100 for TIC; 2375 for alkalinity; 0.16 for chlorophyll-a; 0.013 for DMSPp; 0.1 for DMSPd and DMS; and zero for the remaining variables. The boundary conditions are zero-flux in order to conserve mass (with the exception of sulfur since DMS emission in the upper top grid is allowed). A mass-conservative ecosystem model is desirable so that the biotic pools do not eventually run out of nutrients [*Spitz et al.*, 2001; *Cropp et al.*, 2004]. An accumulation of dying phytoplankton and detritus in the bottom boundary due to vertical sinking occurs, which implies that DOM increases and finally that NH_4^+ and NO_3 = (from NH_4^+ nitrification) also accumulates. This simulates the observed presence of high NO_3 = levels deep in the water column at BATS [*Steinberg et al.*, 2001]. During winter, the MLD reaches the bottom and the strong mixing carry some of this nutrients pool to the UML, generating the vernal phytoplankton bloom (see section 3. Results and Discussion). In order to reach an equilibrium state, the model was ran for 10 years (with a time step of 0.005 days) prior to the analysis of the results. Previous tests

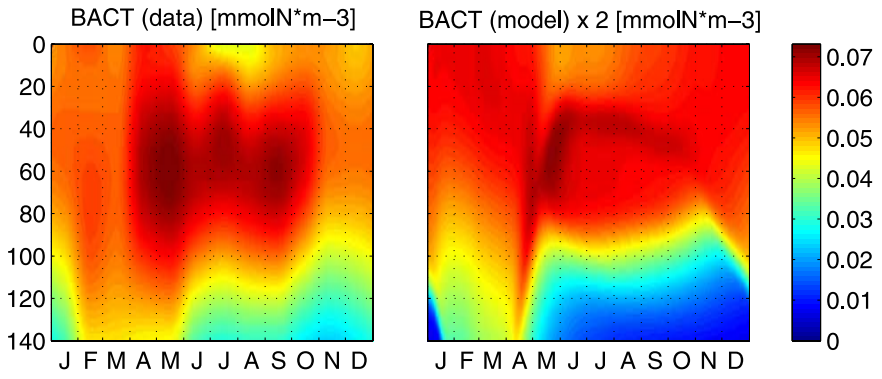

Figure 2. Two-dimensional (time, depth) plots of bacteria (mmolN m^{-3}) from climatological in situ data (left) and DMOS model results (right). Conversion from bacterial counts (10^8 cells kg^{-1}, BATS data) to mmolN m^{-3} was done using a conversion factor of 0.0118 (mmolN $m^{-3}/10^8$ cells kg^{-1}), which was obtained assuming that bacterial cells have 7.2 fgC $cell^{-1}$ [*Gundersen et al.*, 2002] and a C:N molar ratio of 5.1 (Table 1). Note that simulated bacteria are scaled up by a factor of 2 for the sake of visual comparison against data.

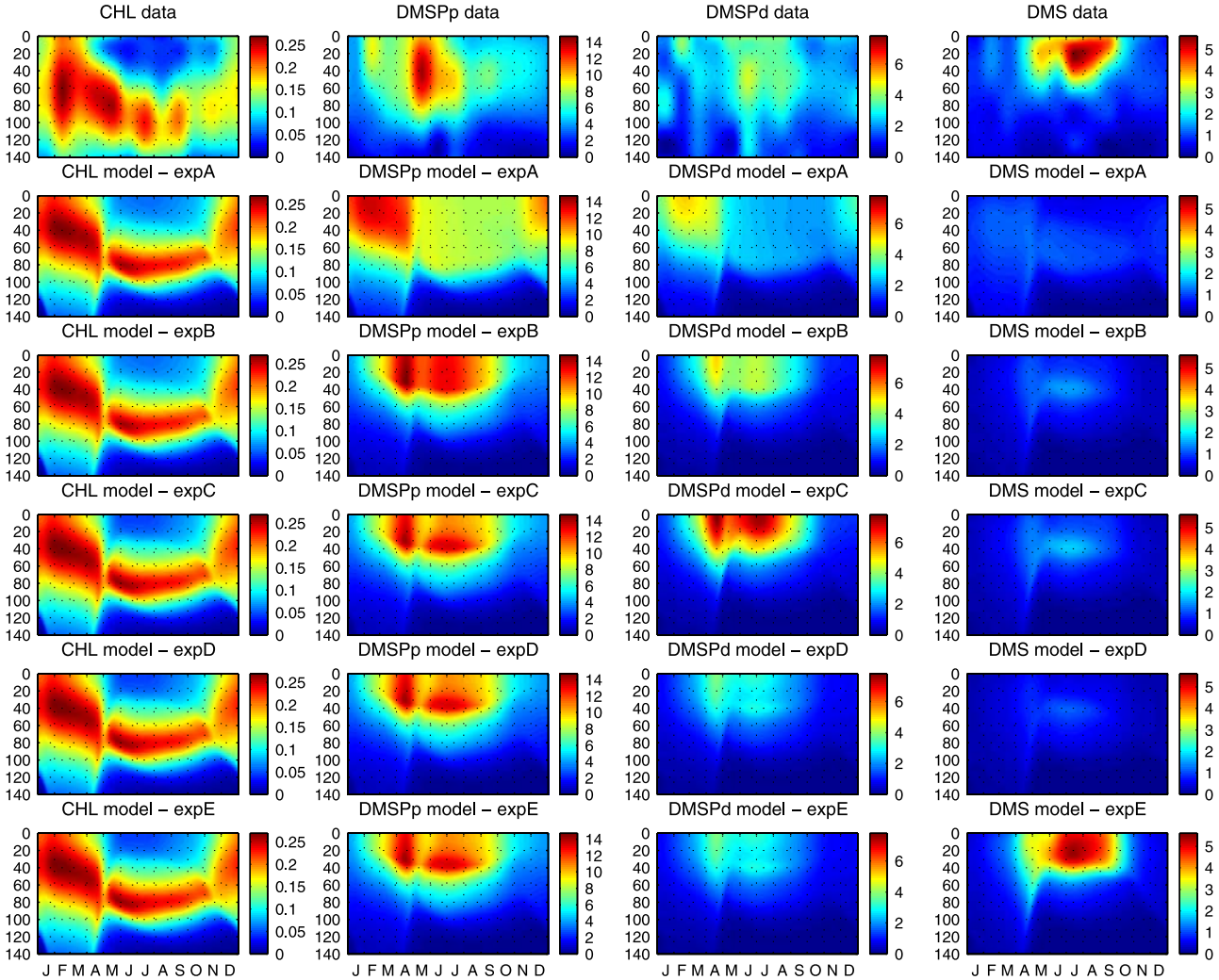

Figure 3. Two-dimensional (time, depth) plots of chlorophyll-a, DMSP particulate, DMSP dissolved and DMS from climatological in situ data (upper-row panels) and DMOS model results for several modeling experiments (see Table 2): experiment A (second-row panels), experiment B (third-row panels), experiment C (fourth-row panels), experiment D (fifth-row panels), experiment E (sixth-row panels). Units: chlorophyll-a (mg m^{-3}), DMSPp-DMSPd-DMS (μmolS m^{-3}).

Table 2. Model Experiments

Process Affecting S-Cycle	ExpA	ExpB	ExpC	ExpD	ExpE
Phyto. S:N ratio shift by UV:	NO	YES	YES	YES	YES
Bact. inhibition by UV:	NO	NO	YES	YES	YES
Phyto. DMSPd consumption:	NO	NO	NO	YES	YES
Phyto. DMS production by UV:	NO	NO	NO	NO	YES

without seasonal forcings showed that the model reaches a "stable node" equilibrium, indicating that the model does not have unwanted internal dynamics (e.g. oscillations) and that the seasonal changes are driven by the seasonal forcings.

3. Results and Discussion

[23] The model successfully reproduces bacteria (Figure 2) and CHL (Figure 3) distributions, capturing the winter/spring phytoplankton bloom in surface and the deep chlorophyll maximum (DCM) during summer months (Figure 3) as well as the development of a subsurface maximum (40–60 m depth) of bacteria from late spring to early fall (Figure 2). Modeled values of bacteria concentrations are, however, about a half those of the data. This is because the model only simulates active bacteria, while the data includes both active and nonactive bacteria [*Anderson and Pondaven*, 2003]. The vernal phytoplankton bloom is triggered by the entrainment of deep nutrients. In contrast, nutrients are depleted in summer leading to lowest phytoplankton biomass in surface waters. Deeper in the water column, the presence of higher concentrations of nutrients along with light in sufficient quantity for primary production results in the formation of a DCM. Bacteria distributions mainly result from the interplay of DOM release by phytoplankton and the inhibition of bacterial DOM uptake by high solar radiation doses during summer.

3.1. Model Experiments

[24] In order to gain some insight into the processes that are most relevant for explaining the observed seasonality of DMS in the Sargasso Sea, and therefore what drives the DMS summer paradox, we conducted several model experiments turning "off" or "on" various DMOS sulfur paths. This exercise was undertaken in a sequence of steps, starting from the simplest characterization of the S-cycle and increasing complexity in a stepwise fashion until realistic simulations were obtained. The first scenario excluded all of the processes usually cited in the literature to explain the DMS summer paradox, namely shift in the S:N ratio of phytoplankton, inhibition of bacterial uptake by UV light, phytoplankton uptake of DMSPd, and phytoplankton exudation of DMS under UV stress. Each of these processes was then added one after the other (see Table 2). Simulations for each of the experiments (A, B, C, D, E; Table 2) are compared with observations for the Sargasso Sea observations (0–140 m) in Figure 3.

3.1.1. Experiment A

[25] In this experiment there is no seasonal increase in the S:N ratio of phytoplankton (therefore $\theta_{Ps:n}$ is constant and equal to 0.13 mmolS mmolN^{-1}, the middle value between $\theta^{\min}_{Ps:n}$ and $\theta^{\max}_{Ps:n}$), UV induces neither bacterial inhibition of semilabile-DOM/NH_4^+ and sulfur uptake (DMSPd and DMS) nor phytoplankton stress-driven DMS production, and phytoplankton does not to take up DMSPd. Modeled DMSPp, DMSPd and DMS closely follow the predicted CHL distribution, all displaying maximum values in winter/spring and minima in summer/fall (Figure 3). The main differences between DMSPp and CHL are due to the variability of CHL as a response of the levels of light intensity. This constancy between sulfur species and CHL is not observed in the data. Further, DMSPp maximum values are slightly underestimated while DMS values are highly underestimated. We must conclude that this experiment is not capturing at all the main processes controlling oceanic sulfur dynamics.

3.1.2. Experiment B

[26] In contrast to the previous experiment, a variable S:N internal quota in phytoplankton was now added in order to parameterize a seasonal change in species composition towards high DMSPp producers and/or a change in phytoplankton physiological state due to higher UV doses [*Sunda et al.*, 2002; *Slezak and Herndl*, 2003]. Results are shown in Figure 3. The simulations for DMSPp are improved in comparison to the first experiment. However, the modeled DMSPp maximum in spring takes place earlier than observed (by about one month, similar to what was observed by [*Le Clainche et al.*, 2004]) and DMSPd distributions correlate too closely with DMSPp, a feature not observed in the field [*Dacey et al.*, 1998]. DMSPp simulations are also clearly overestimated during summer. Therefore, the parameterization of the S:N ratio as a function of light, although better than using a constant value, is far from being perfect. There is a need to explore other ways of modeling DMSPp concentrations, e.g., by including in the model several phytoplankton groups with specific S:N internal quotas. On the other hand, DMS values are again severely underestimated and, although a summer maximum is now predicted, it is deeper in the water column and smaller in magnitude than seen in the observations. Furthermore, predicted DMS in surface waters does not display the summer maximum seen in the observations, but rather shows a spring maximum. It therefore appears that inclusion of a variable the S:N ratio of phytoplankton in the model can not on its own account for the observed seasonality of DMS nor explain the DMS summer paradox.

3.1.3. Experiment C

[27] Next, the inhibition of bacterial uptake of nutrients (semilabile-DOM/NH_4^+) and sulfur (DMSPd and DMS) by solar radiation was added to the model [*Herndl et al.*, 1993; *Slezak et al.*, 2001; *Toole et al.*, 2006]. This fact has been also cited as a potential explanation for the DMS summer paradox since a reduction in a major sink may cause DMS to accumulate [*Simó and Pedrós-Alió*, 1999; *Simó*, 2001, 2004]. Model results (see Figure 3) indicate that inhibition of bacterial sulfur uptake by UV could partly explain the

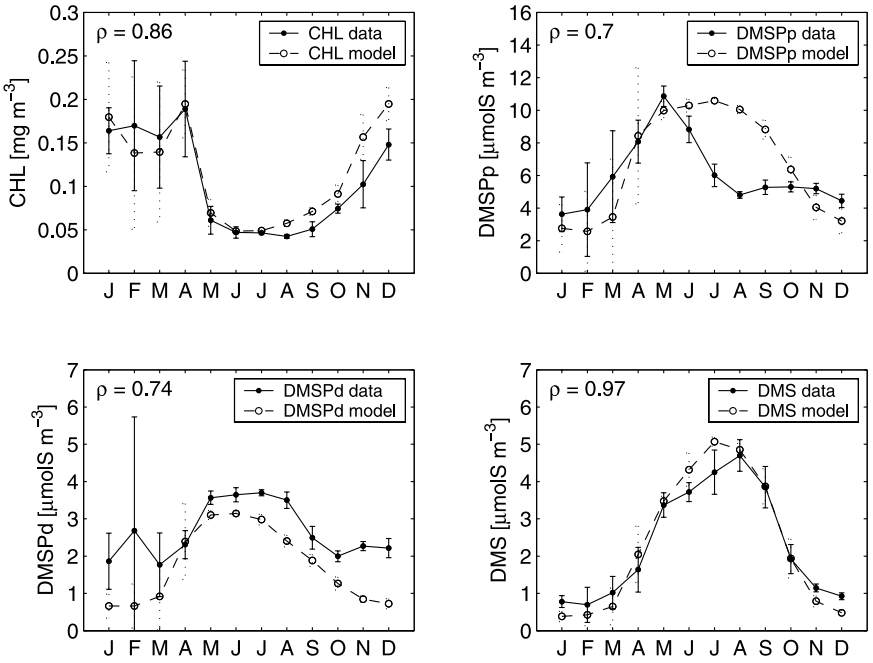

Figure 4. Monthly upper mixed-layer averaged values of chlorophyll-a, DMSP particulate, DMSP dissolved and DMS for climatological in situ data (solid line) and DMOS model results (dashed line) for Experiment E. Units: chlorophyll-a (mg m^{-3}), DMSPp-DMSPd-DMS (μmolS m^{-3}).

cause of the deep summer maximum of DMS, although the predicted maximum is slightly deeper than in the observations and DMS values remain underestimated. However, DMS accumulation occurs in conjunction with an unrealistically large accumulation of DMSPd. This overestimate in modeled DMSPd may be due to the absence in the model of phytoplankton uptake, a new sink for DMSPd that has been recently discovered experimentally [*Vila-Costa et al.*, 2006b]. The DMSPd accumulation implies a large contribution to DMS from free DMSP-lyases (1% of the DMSPd pool is converted into DMS each day). We therefore have repeated experiments B and C, but without free DMSP-lyases activity to evaluate if inhibition of bacterial sulfur uptake by UV can produce this DMS accumulation. Results (not shown) displayed a very weak increase of the deep DMS maximum in summer (much weaker than the increase observed from experiment B to experiment C, see Figure 3), not enough to be the origin of the DMS summer paradox. This result is a consequence of the fact that, although bacterial DMS uptake is reduced by the UV-induced inhibition (which tends to increse DMS), there is also a reduction of bacterial DMS production (from the associated inhibition of DMSPd uptake). The net balance of these two opposite effects is almost zero.

3.1.4. Experiment D

[28] The next process added to the model was consumption of DMSPd by phytoplankton. It has been reported recently that some groups of phytoplankton (diatoms and cyanobacteria) are able to take up DMSPd [*Vila-Costa et al.*, 2006b]. This process may help explain the low values of DMSPd observed in the field and the strong decoupling of DMSPd to either DMSPp or DMS [*Dacey et al.*, 1998]. The resulting simulations (see Figure 3) show an improvement in predicted DMSPd concentrations, although spring values are still overestimated relative to the observations. On the other hand, modeled DMS is totally unsatisfactory, with values clearly underestimated and showing a very weak deep summer maximum.

3.1.5. Experiment E

[29] The next addition to the model was a direct exudation term of DMS from phytoplankton cells as a response to UV-induced stress [*Sunda et al.*, 2002; *Toole and Siegel*, 2004]. Direct DMS production by phytoplankton has been reported previously in the literature [*Vairavamurthy et al.*, 1985; *Niki et al.*, 2000, and references therein; *Wolfe et al.*, 2002]. This DMS production, therefore, is not routed through the DMSPd pool but comes directly from the DMSPp (in the model it is assumed that the amount of DMS exuded from the cells is immediately replaced by newly produced DMSPp). The results of this experiment, which incorporates all the mechanisms thought to be important in the sulfur cycle of the ocean, show a clear improvement over those of the previous experiments and also of existing DMSP/DMS models. Simulated DMS now shows good agreement with the observations (see Figure 3), with a summer maximum of about 5 μmolS m^{-3} at around 20 m depth and winter minima of about 0.5 μmolS m^{-3}. The predicted summer DMS maximum occurs below the surface because of the high DMS photolysis and ventilation rates occurring in the upper layers. The results suggest that phytoplankton DMS exudation may be an important factor contributing to the high summer to winter ratio of DMS concentrations observed in the field as well as explaining the strong decoupling between CHL and DMS.

3.2. Further Analysis of Experiment E

[30] Results from the series of experiments described above indicate that the various mechanisms involved in

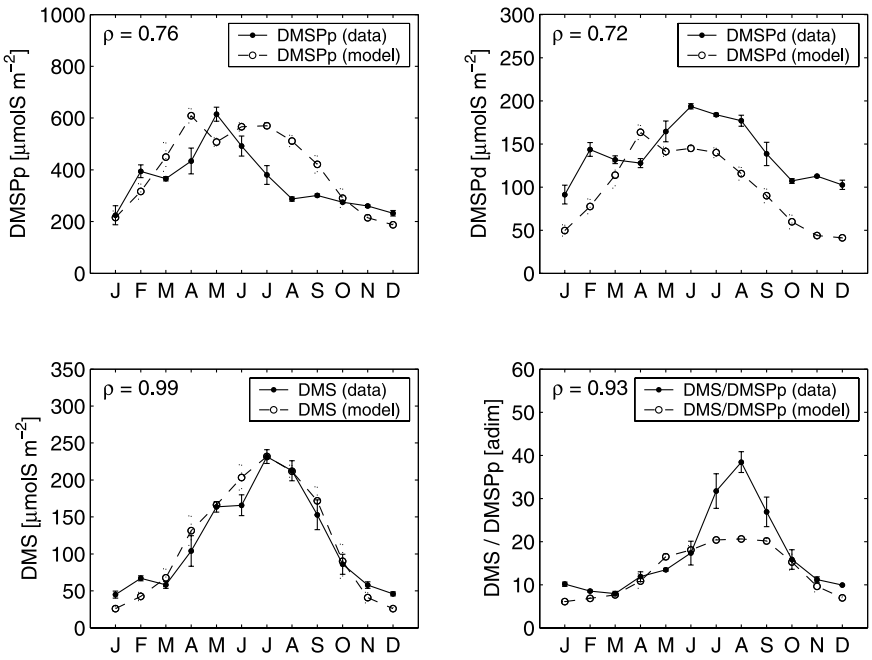

Figure 5. Monthly upper 50 m-integrated values of DMSP particulate, DMSP dissolved, DMS and DMSPp/DMS ratio for climatological in situ data (solid line) and DMOS model results (dashed line) for Experiment E. Units: DMSPp-DMSPd-DMS (μmolS m^{-2}).

the S-cycle (seasonal variations in the internal S:N quota, bacterial inhibition of sulfur uptake, exudation of DMS as well as DMSPd uptake by phytoplankton) all can play a role in driving the DMS seasonality. The direct exudation of DMS from phytoplankton cells (as a response of high UV doses) does however appear to be a major one: without this process the model is unable to realistically reproduce the observed DMS cycle and thereby explain the summer paradox.

[31] Monthly UML averages of CHL, DMSPp, DMSPd and DMS (data and model) are shown in Figure 4, along with their associated (Spearman) correlation coefficients. In general, the model is able to realistically capture both the seasonality and the absolute magnitude of these four variables. The main discrepancies between the model and the observations are that model summer DMSPp values are clearly overestimated (by as much as a factor of two in August) and that DMPSd values are slightly underestimated in the model. In this regard, however, experimentalists believe that past and current DMSPd measurements are likely to be overestimates due to filtration artifacts [*Kiene and Slezak*, 2006].

[32] Examination of the 50-m depth integrated values for DMSPp, DMSPd, DMS and the DMS:DMSPp ratio (Figure 5) leads to similar conclusions. The model does a reasonably good job at reproducing the sulfur variables, although the predicted DMSPp maximum occurs one month too early and predicted DMSPp concentrations are generally too high. On the other hand, DMSPd values are underestimated in summer. Both modeled DMS and data display maxima in July, showing good agreement both in magnitude and seasonality. Due to the predictions of DMSPp being too high in August, the modeled DMS/DMSPp ratio is, however, markedly underestimated for this month.

[33] The vertically resolved seasonal cycles of predicted sulfur fluxes in the model are shown in Figure 6. Bacterial uptake of DMSPd (Figure 6a) is highest in spring and summer (e.g., more than $\approx$1.5 μmolS m^{-3} d^{-1} occurred at depths between 20 m and 60 m) coincident with high modeled bacterial biomass (see Figure 2) and DMSPd concentrations (see Figure 3). Uptake rates decline thereafter until an annual minimum is reached in winter. Phytoplankton uptake of DMSPd (Figure 6b) displays a similar seasonality, with an annual maximum in spring ($\approx$1.5 μmolS m^{-3} d^{-1} in April) and a secondary maximum during summer ($\approx$1.0 μmolS m^{-3} d^{-1}) for surface waters (<30 m). Bacterial uptake of DMSPd is in general higher than that of phytoplankton, and has a broader and deeper distribution (values higher than 1 μmolS m^{-3} d^{-1} reach depths of about 80 m while phytoplankton uptake does not occur deeper than 40 m).

[34] Bacterial uptake of DMS (Figure 6c) is highest in summer at depths between 20 m and 40 m, reaching values of 0.5 μmolS m^{-3} d^{-1}. In July 2004, *del Valle et al.* [2007] reported a maximum DMS consumption rate of $\approx$0.8 μmolS m^{-3} d^{-1} around 40 m depth. In surface waters in summer, bacterial uptake rates of both DMSPd and DMS (Figures 6a and 6c) are reduced by almost a half due to UV-induced bacterial inhibition. Minimum bacterial DMS uptake occurs during winter due to the very low DMS concentrations. Relatively low bacterial DMS consumption rates (0.3 μmolS m^{-3} d^{-1}) were measured in the Sargasso Sea in May at the DCM by *Levasseur et al.* [2004]. Similar rates (0.2–0.3 μmolS m^{-3} d^{-1}, see Figure 6c) are predicted in the model in May between 60–80 m (the depth of modeled DCM, see Figure 3).

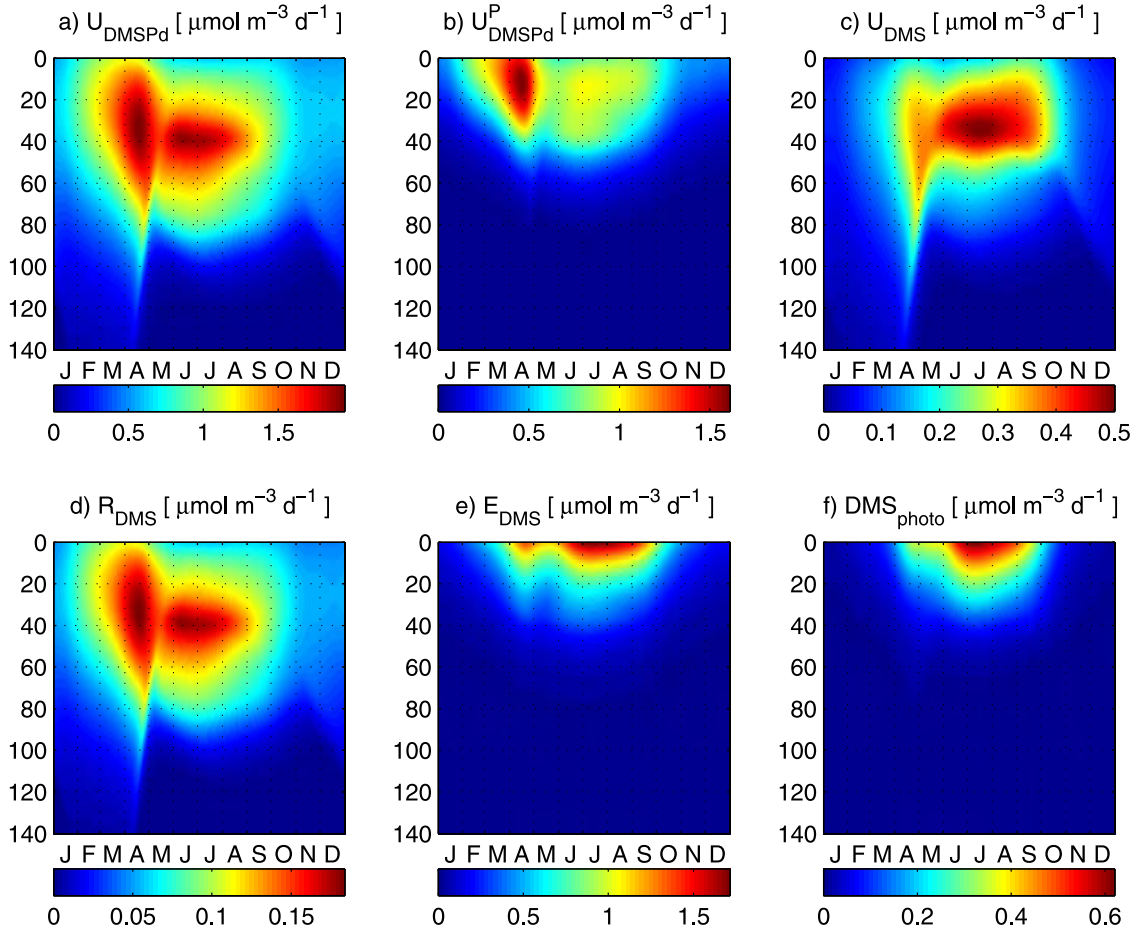

Figure 6. Two-dimensional (time, depth) plots of DMOS model sulfur fluxes (μmolS m^{-3} d^{-1}) for Experiment E: (a) Bacterial uptake of DMSP dissolved. (b) Phytoplankton uptake of DMSP dissolved. (c) Bacterial uptake of DMS. (d) Bacterial production of DMS. (e) Phytoplankton production of DMS. (f) Photolysis of DMS.

[35] The predicted bacterial production of DMS by enzymatic cleavage of DMSPd (Figure 6d) follows the DMSPd uptake (Figure 6a) and represents approximately 8–9% of the former, in agreement with estimates for the Northern Sea (6–12% [see *Zubkov et al.*, 2002]). Maximum values (higher than $\approx$0.15 μmolS m^{-3} d^{-1}) therefore are obtained in spring and summer at depths between 20 m and 60 m. On the other hand, DMS production from phytoplankton exudation (Figure 6e) displays its highest values in summer at the very surface, reaching rates of more than 1.5 μmolS m^{-3} d^{-1} in July. Since this process is light-driven, the values increase exponentially towards the surface. The sum of phytoplankton exudation and bacterial DMS production gives a higher gross biological production in summer (up to 1.8 μmolS m^{-3} d^{-1}, not shown) in the UML. In spring, the modeled gross biological production of DMS at the surface is about 1.4–1.6 μmolS m^{-3} d^{-1}, a value in good agreement with in situ data from the Sargasso Sea (1.8 μmolS m^{-3} d^{-1}, [*Levasseur et al.*, 2004]). In a separate short-term study, where a mass balance assumption was applied to measured rates, light-mediated biological DMS production rates as high as 8 μmolS m^{-3} d^{-1} were estimated by *Toole et al.* [2006]. There is such a scarcity of in situ measurements addressing this issue that future field work is needed. DMS photolysis (Figure 6f) also reaches a maximum in summer (up to 0.6 μmolS m^{-3} d^{-1} in July) as a consequence of maximum DMS concentrations and light exposure. *Toole et al.* [2003] estimated maximum UML-integrated DMS photolysis rates in summer of about 10–15 μmolS m^{-2} d^{-1}. These estimates were based on a summer MLD of $\approx$20 m. For this MLD value, our integrated DMS photolysis rates in summer are very similar (10–12 μmolS m^{-2} d^{-1}).

[36] Model sulfur fluxes averaged over the UML are shown in Figure 7. Bacterial and phytoplankton uptake of DMSPd are similar in magnitude (Figures 7a and 7b, respectively) as are bacterial DMS consumption and DMS photolysis (Figures 7c and 7f). On the other hand, predicted phytoplankton DMS exudation can be an order of magnitude higher (e.g. in summer) than bacterial production (Figures 7e and 7d, respectively).

[37] Turnover rates of DMSPd and DMS due to bacterial consumption, phytoplankton DMSPd uptake, and DMS photolysis are shown in Figure 8. Turnover rate (or rate constant, d^{-1}) is the process rate (μmolS m^{-3} d^{-1}) divided by the concentration (μmolS m^{-3}). Maximum turnover rates, thus lower turnover times (1/turnover rates, d), due

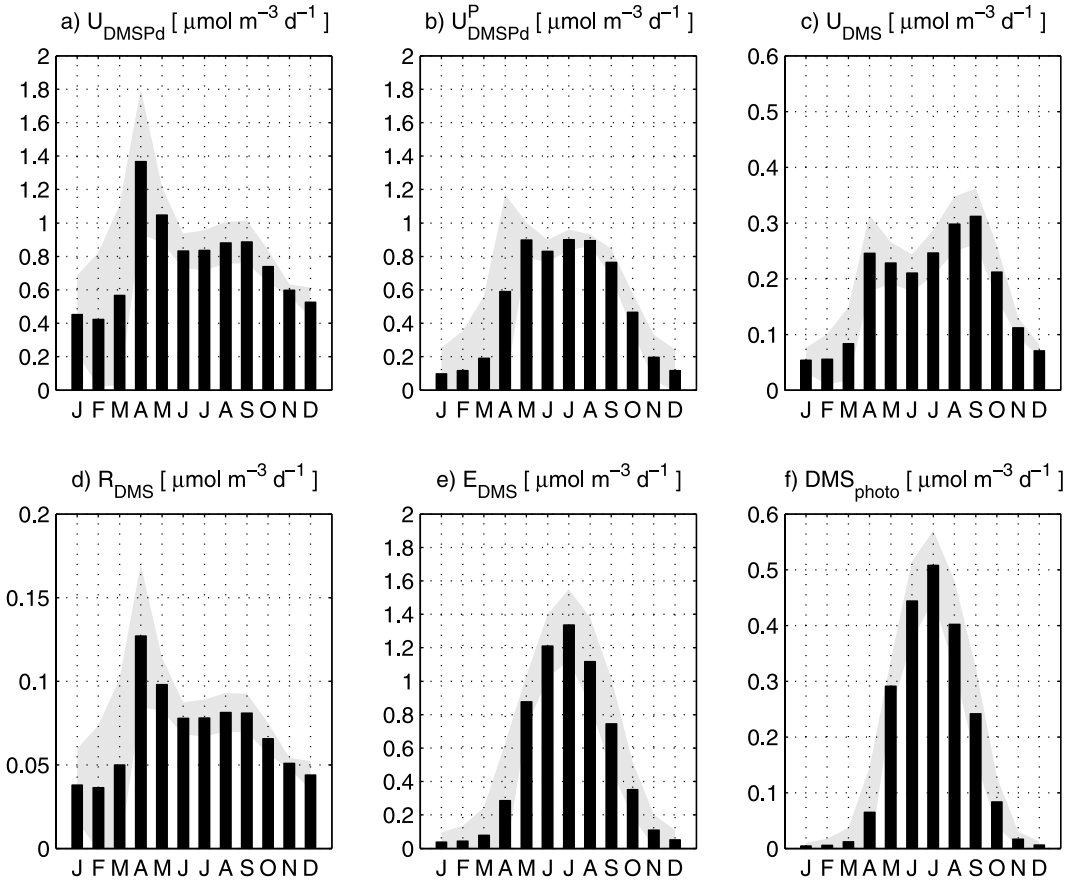

Figure 7. Monthly upper mixed-layer averaged values of DMOS model sulfur fluxes (μmolS m^{-3} d^{-1}) for Experiment E: (a) Bacterial uptake of DMSP dissolved. (b) Phytoplankton uptake of DMSP dissolved. (c) Bacterial uptake of DMS. (d) Bacterial production of DMS. (e) Phytoplankton production of DMS. (f) Photolysis of DMS. The gray shadow area represents the standard deviation of the averages.

to bacterial uptake are obtained at depth (between 20–60 m in winter and 60–80 m in summer) both for DMSPd and DMS (Figures 8a and 8c, respectively). Bacterial inhibition of sulfur uptake by UV at the surface is observed in summer. Turnover rates of DMS are about 20% of those for DMSPd because only this percentage of bacteria was assumed to be DMS consumers (see section 2.2. Model Description). Thus, minimum turnover times for bacterial consumption of DMSPd and DMS are estimated as ≈1.5 and ≈6 days, respectively. Bacterial turnover rates of DMSPd and DMS have also been observed to be highest in subsurface waters of the North Sea during a coccolithophore bloom (although they were nevertheless about an order of magnitude higher than our results) [*Zubkov et al.*, 2001, 2002]. For the Sargasso Sea, DMSPd and DMS turnover times have been estimated to vary between 0.4–2.8 days and <0.5–8 days respectively [*Ledyard and Dacey*, 1996].

[38] Predicted rates of phytoplankton DMSPd turnover (Figure 8b) are of the same order of magnitude (yet slightly lower) than those of bacterial uptake (Figure 8a). Their vertical distribution is however very different because phytoplankton uptake depends on primary production and hence is only significant in irradiated waters (<40 m). Maximum values are present in spring due to the highest primary production. Total DMSPd turnover rates (bacterial and phytoplankton uptakes plus free DMSP-lyases activity) for the upper 50 m are in the range of 0.5–1.0 d^{-1} (not shown), in good agreement with the values reported by *Ledyard and Dacey* [1996] for the Sargasso Sea (0.7–1.5 d^{-1}, see Table 2 in *Kiene and Linn* [2000]). Maximum turnover rates of DMS photolysis (Figure 8d) are about 75% of the maximum rates of bacterial consumption (Figure 8c). Highest photolysis rates are, however, mainly concentrated in the upper 20 m in summer, a layer and period where bacterial consumption is low. Photolysis then dominates the loss of DMS in the upper ocean, while bacterial consumption dominates at greater depths [*Toole et al.*, 2006; *Kieber et al.*, 1996].

[39] Turnover rates averaged for the UML are shown in Figure 9. UML DMS turnover rates are between 0.05 and 0.15 d^{-1}. For a 60 m mixed water column in the equatorial Pacific, *Kieber et al.* [1996] obtained bacterial DMS turnover rates of 0.04–0.66 d^{-1}. In the Sargasso Sea, bacterial DMS consumption rates in September were estimated to be ≈0.5 μmolS m^{-3} d^{-1} [*Lefevre et al.*, 2002, and references therein]. For that month UML averaged DMS concentration from the data is about 4.0 μmolS m^{-3} (see Figure 4), giving a specific rate of 0.12 d^{-1}, similar in magnitude to the model results (≈0.08 d^{-1}, see September in Figure 9c). An interesting feature emerging from the model results is that

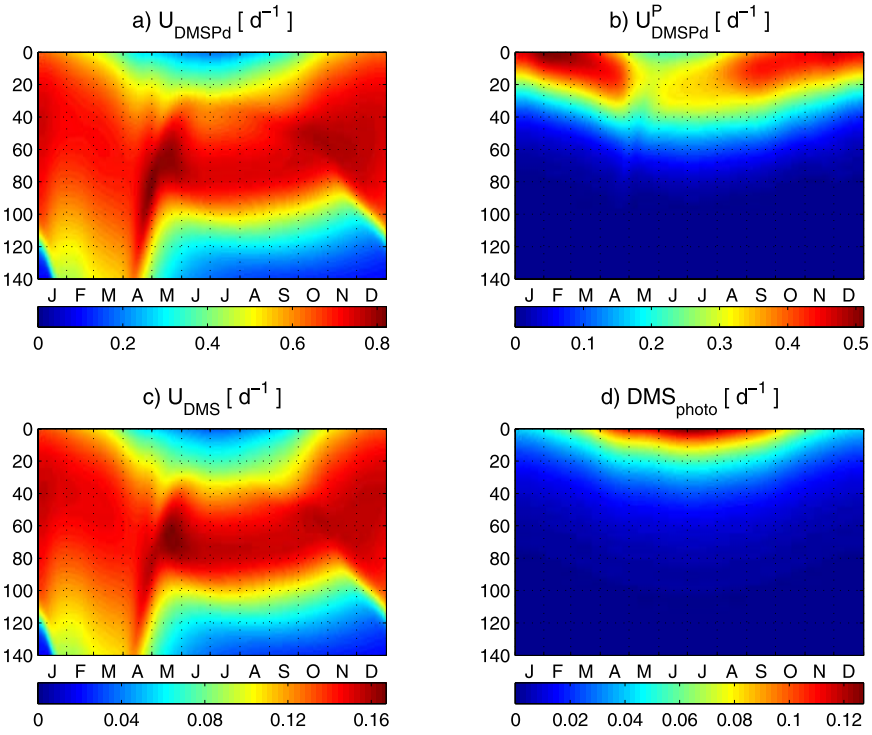

Figure 8. Two-dimensional (time, depth) plots of DMOS model sulfur turnover rates (d^{-1}) for Experiment E: (a) Bacterial uptake of DMSP dissolved. (b) Phytoplankton uptake of DMSP dissolved. (c) Bacterial uptake of DMS. (d) Photolysis of DMS.

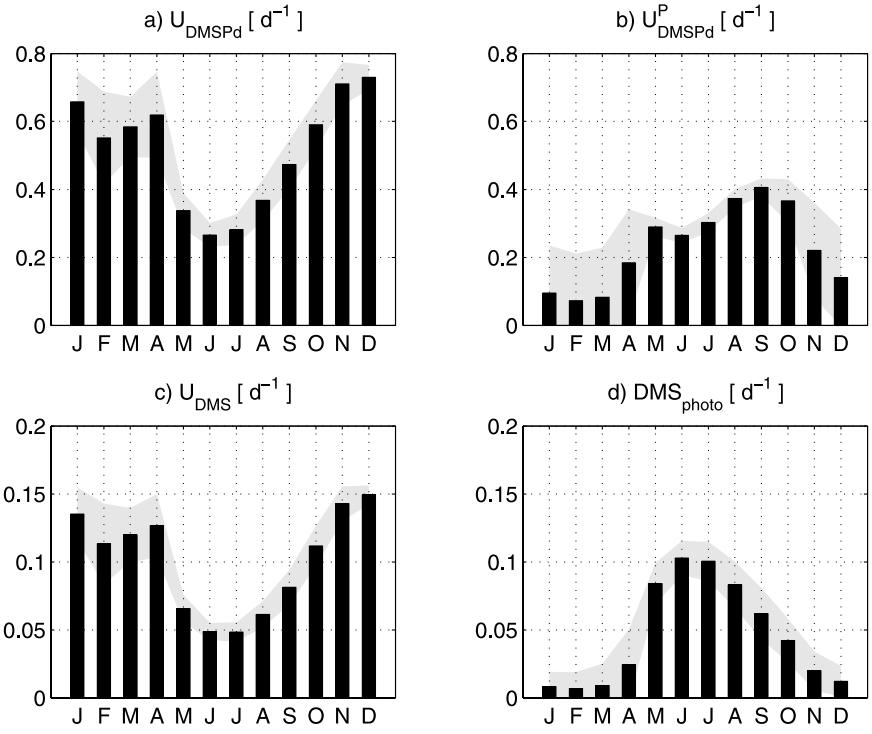

Figure 9. Monthly upper mixed-layer averaged values of DMOS model sulfur turnover rates (d^{-1}) for Experiment E: (a) Bacterial uptake of DMSP dissolved. (b) Phytoplankton uptake of DMSP dissolved. (c) Bacterial uptake of DMS. (d) Photolysis of DMS. The gray shadow area represents the standard deviation of the averages.

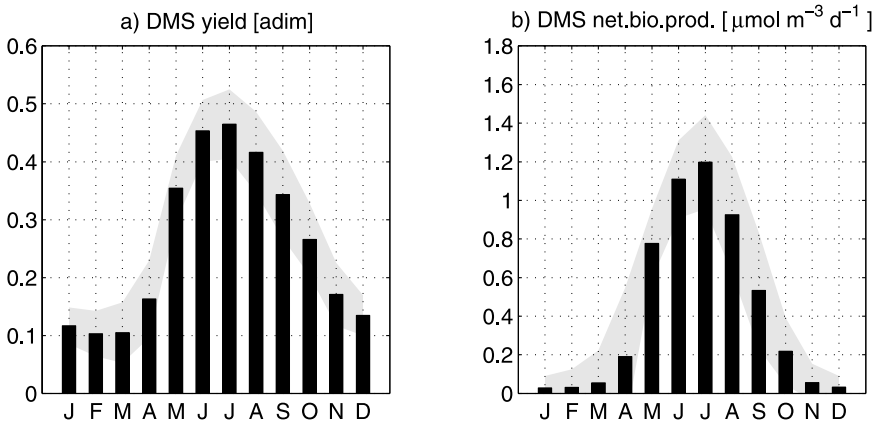

Figure 10. Monthly upper mixed-layer averaged values of: (a) DMS yield (DMS production/DMSP consumption). (b) Net biological DMS production (DMS production - bacterial uptake of DMS). The gray shadow area represents the standard deviation of the averages.

bacterial DMS consumption is the dominant loss term in winter and spring (Figure 9c), while in summer it is DMS photolysis (Figure 9d), as postulated previously [*Toole et al.*, 2006].

[40] We calculated the DMS-yield (equation (A79)) for the whole food web (total DMS production divided by total DMSP consumption) from the model sulfur fluxes, as well as the net biological production of DMS (total DMS production minus bacterial DMS consumption) averaged over the UML (see Figure 10). The DMS-yield (Figure 10a) displays a clear seasonal pattern with higher values during summer (up to ≈45%) and lower values in winter (≈10%). For both variables the annual maximum is observed in July. These values are in the range reported in the literature [*Simó and Pedrós-Alió*, 1999]. Net biological production of DMS (Figure 10b) follows the same seasonality, increasing from almost zero to ≈1.2 μmolS m^{-3} d^{-1} in summer. Very similar values and seasonality of net biological production of DMS were estimated by *Toole and Siegel* [2004], based on the same set of data, when using a mass-balance model (from zero in winter to 1.0–1.5 μmolS m^{-3} d^{-1} in summer).

[41] Since DMS fluxes to the atmosphere are believed to have a role in regulating climate [*Charlson et al.*, 1987; *Andreae and Crutzen*, 1997], we plotted them along with UML DMS emission rates (DMS flux divided by the MLD) and surface DMS concentrations (upper top cell grid) (see Figure 11). The highest values of the three variables occur in summer (June, July, August). In particular, DMS flux to the atmosphere shows a clear maximum in July (≈12 μmolS m^{-2} d^{-1}). The UML is exposed to very high doses of solar radiation during this month (because of the high solar incident radiation and very shallow MLD). If the proposed antioxidant function of DMS [*Sunda et al.*, 2002] as well as the impact of DMS on CCN and Earth albedo are shown to be important, then this higher DMS flux to the atmosphere in summer could act as a negative feedback between the ocean's ecosystems and the amount of solar radiation reaching the ocean's surface [*Charlson et al.*, 1987; *Vallina and Simó*, 2007; *Vallina et al.*, 2007]. Maximum DMS emissions from the UML (June/July; ≈1.0 μmolS m^{-3} d^{-1}) are about a factor of two and four higher than the summer DMS losses by photolysis or bacterial consumption respectively (≈0.5 and ≈0.25 μmolS m^{-3} d^{-1}; see Figures 7c and 7f).

3.3. Sensitivity Analysis

[42] In order to evaluate the sensitivity of model results to model parameters values we carried out a sensitivity analysis (SA) by increasing/decreasing each parameter by 50% in each run and comparing the results to the control simulation (experiment E, Table 1 with the exception of parameters δ_1, α_1 and ϕ_{inhib}^{max} that were lowered to 0.5 in the reference control to allow an increase of 50%). The SA index was taken from *Le Clainche et al.* [2004] and is defined as follows:

$$S_k = \frac{X_{k_{\max}} - X_{k_{\min}}}{X_{k_{control}}} * 100 \quad (1)$$

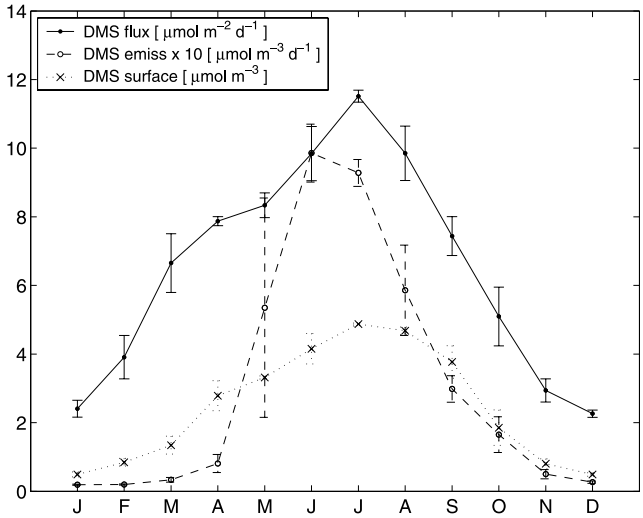

Figure 11. Monthly averaged values and standard deviation of surface DMS (μmolS m^{-3}, dotted line), DMS ventilation flux (μmolS m^{-2} d^{-1}, solid line), upper mixed layer DMS ventilation (defined as DMS flux/MLD) (10*μmolS m^{-3} d^{-1}, dashed line).

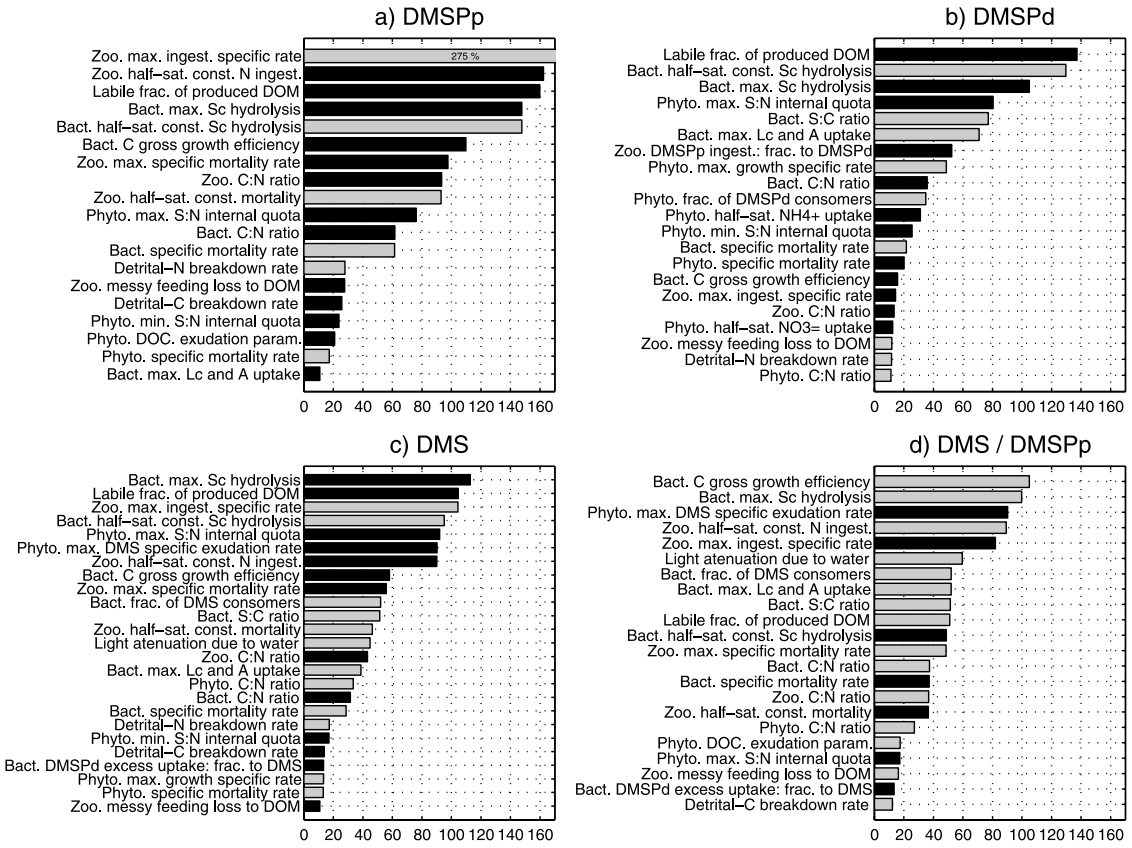

Figure 12. Sensitivity analysis indices of the DMOS model to changing parameters by ±50%. Black bars indicate that an increase of the parameter causes an increase of the variable, while grey bars indicate that an increase of the parameter causes a decrease of the variable.

where $X_{kcontrol}$, $X_{k\max}$ and $X_{k\min}$ are the annual budgets of DMSPp, DMSPd and DMS integrated over the upper 50m obtained for the 3 simulations: control (reference value of the parameter k), 50% increase in the parameter k ($k_{\max}$ = 1.5k), and 50% decrease in the parameter k ($k_{\min}$ = 0.5k) [*Le Clainche et al.*, 2004]. Only those parameters which gave SA indices greater than 10% are plotted in Figure 12. Black bars indicate that an increase of the parameter results in an increase in the state variable, while grey bars indicate that an increase in the parameter produced a decrease in the state variable.

[43] For DMSPp (Figure 12a) we observe that parameters related to zooplankton grazing have the largest effects, mainly the maximum zooplankton specific ingestion rate. This is not surprising since they directly affect the phytoplankton biomass. Another important parameter is the labile fraction of DOM produced. Other SA tests (not shown) revealed that this parameter is a key one for the nutrient pools due to the bacterial microbial loop; an increase of DOM concentrations is associated to a rise of $NO_3^=$ and NH_4^+ in the model, and thus to an increase of modeled phytoplankton. Bacterial hydrolysis of semilabile DOM and gross growth efficiency are also very important because they affect the amount of labile DOM (and then again the nutrient pools and phytoplankton biomass). Parameters related to zooplankton mortality are associated to DMSPp through the levels of grazing activity upon phytoplankton, while the zooplankton C:N ratio affects the DOC pool (and again the microbial loop). Interestingly, the maximum S:N internal quota of phytoplankton is not the most important parameter contrary to the results of *Lefevre et al.* [2002] and *Le Clainche et al.* [2004]. This difference is in part attributable to the fact that in the SA carried out by these authors they increased/reduced by 50% the minimum and maximum S:N internal ratios at the same time, while we have increased/reduced them separately. Nevertheless, these results suggest that bottom-up (nutrient availability, regulated by the microbial loop) and top-down (zooplankton grazing) processes that control phytoplanktom biomass are more important for DMSPp concentrations than the internal sulfur quota.

[44] For DMSPd (Figure 12b), the 10 most sensitive parameters are related to the microbial loop, except for the maximum phytoplankton internal S:N quota (4th position), the bacterial S:C ratio (5th position), the fraction of ingested DMSPp by zoo that is recovered as DMSPd (7th) and the phytoplankton maximum specific growth rate (8th).

[45] Regarding DMS (Figure 12c), we observe a set of seven parameters that have a consistently high influence (from ≈90% to from ≈110%), clearly larger than the rest (<60%). With the exception of the maximum phytoplankton S:N internal quota (5th position) and the maximum phytoplankton DMS exudation specific rate (6th position), all were ranked already in the top five most sensitive parameters for DMSPp (Figure 12a). They are related to the bottom-up and top-down processes controlling phytoplankton biomass previously cited. The parameter for the fraction

of bacteria that is DMS consumers is ranked on the 10th position, which is significant since at present this is an uncertain parameter. It is followed by the bacterial S:C ratio. A higher S:C ratio implies higher sulfur requirements of bacteria (lower DMS production from DMSPd uptake) at the same time than higher DMS uptake. There is large variation in published values for the S:C molar ratio ranging from ≈1/50 to ≈1/250 [*Zubkov et al.*, 2002, and references therein]. Further research is needed in order to better constrain this parameter. As expected, the light attenuation coefficient is also quite important (13th position) because any increase reduces the amount of DMS exudation by phytoplankton. On the other hand, increasing it also reduces the DMS photolysis. However, since DMS exudation by phytoplankton was about 3 times higher than DMS photolysis (see Figure 6), the reduction of the source term dominates.

[46] In order to evaluate which parameters affect DMS concentrations in a way not directly related to changes in phytoplankton biomass (i.e., changes in DMSPp) the SA index was also calculated for the ratio DMS/DMSPp (Figure 12d). As expected the DMS/DMSPp ratio is very sensitive to the maximum phytoplankton DMS exudation rate. Significant increases of the DMS/DMSPp ratio are also observed for higher zooplankton grazing rates. On the other hand, parameters that increase bacteria concentrations (e.g., carbon gross growth efficiency, maximum DOM/NH_4^+ uptake, the labile fraction of DOM produced, the phytoplankton DOC exudation parameter, etc.) are associated with a decrease in the ratio. An increase of the light attenuation coefficient also produces a decrease of the DMS/DMSPp ratio.

4. Conclusions

[47] We have presented a state-of-the-art model of the oceanic sulfur cycle which includes the various processes currently thought to be important in DMSP/DMS dynamics and which resolves explicitly DOM and bacteria dynamics within the ecosystem. Sensitivity analyses have shown that parameters related to the microbial loop have a great impact on the N/C/S-cycles, in agreement with previous conclusions reached by both modeling and experimental studies [*Spitz et al.*, 2001; *Simó et al.*, 2000]. The model is able to reproduce the seasonal DMS summer paradox observed in the Sargasso Sea and highlights that bacterial consumption of DMSPd to give DMS may not be the main process in the overall DMS budget. Field studies have also shown that DMS concentrations were not controlled by DMSPd uptake by bacteria [*Dacey et al.*, 1998; *Zubkov et al.*, 2002]. Rather it seems that the key process determining DMS concentrations in the upper ocean may be direct exudation from phytoplankton cells under high UV conditions, this providing an explanation for the strong seasonal decoupling observed between chlorophyll-a and DMS over most of the ocean's surface [*Vallina et al.*, 2006; *Vallina and Simó*, 2007]. This mechanism is missing in all current models of the sulfur cycle, with the exception of the one presented here.

[48] Our model results suggest that DMS production by phytoplankton, despite being only one among several processes that are relevant (such as light-induced increases in the S:N ratio of phytoplankton and light-induced inhibition of bacterial sulfur uptake), is a major contributor to the DMS summer paradox. This has been previously proposed from the analysis of field data in the Sargasso Sea [*Toole and Siegel*, 2004]. The fact that phytoplankton can directly produce DMS has been previously reported in the literature [*Vairavamurthy et al.*, 1985; *Niki et al.*, 2000, and references therein; *Wolfe et al.*, 2002] and there is increasing experimental evidence in support of this claim [*Toole et al.*, 2006]. The implication is that changes in UV levels due to shoaling of the MLD, as might occur in Global Warming scenarios, could have an impact on the oceanic DMS production, and therefore on its potential effect upon Earth climate through CCN formation. Global DMSP/DMS models should incorporate the light-mediated processes affecting DMS production included in DMOS if better estimates of surface DMS concentrations, and specially of its seasonality, are to be achieved.

Appendix A

A1. Model Equations

[49] Phytoplankton [mmolN m^{-3}] equation

$$\frac{\partial P}{\partial t} = (1-\gamma_1)F_P - G_P - M_P - S(P) + D(P) \tag{A1}$$

Zooplankton [mmolN m^{-3}] equation

$$\frac{\partial Z}{\partial t} = F_Z - M_Z + D(Z) \tag{A2}$$

Bacteria [mmolN m^{-3}] equation

$$\frac{\partial B}{\partial t} = F_B - G_B - M_B + D(B) \tag{A3}$$

Nitrates [mmolN m^{-3}] equation

$$\frac{\partial N}{\partial t} = -F_P^N + \nu A + D(N) \tag{A4}$$

Ammonium [mmolN m^{-3}] equation

$$\frac{\partial A}{\partial t} = -F_P^A - \nu A + E_B + E_Z + \Omega_A M_Z + D(Z) \tag{A5}$$

Labile DON [mmolN m^{-3}] equation

$$\frac{\partial L_n}{\partial t} = \gamma_1 F_P + \delta_1[\phi G_n + \varepsilon M_P + M_B + M_{D_n} + \Omega_{dom} M_Z] + U_{S_n} - U_{L_n} + D(L_n) \tag{A6}$$

Labile DOC [mmolC m^{-3}] equation

$$\frac{\partial L_c}{\partial t} = \gamma_1 \theta_{P_{c:n}} F_P + \gamma_1 E_{doc} + \delta_2(1-\gamma_1)E_{doc} + \delta_1[\phi G_c + \varepsilon \theta_{P_{c:n}} M_P + \theta_{B_{c:n}} M_B + M_{D_c} + \Omega_{dom}\theta_{Z_{c:n}} M_Z] + U_{S_c} - \theta_{B_{c:n}} F_B - R_B + D(L_c) \tag{A7}$$

Semilabile DON [mmolN m^{-3}] equation

$$\frac{\partial S_n}{\partial t} = (1-\delta_1)[\phi G_n + \varepsilon M_P + M_B + M_{D_n} + \Omega_{dom} M_Z] - U_{S_n} + D(S_n) \quad \text{(A8)}$$

Semilabile DOC [mmolC m^{-3}] equation

$$\frac{\partial S_c}{\partial t} = (1-\delta_2)(1-\gamma_1)E_{doc} + (1-\delta_1) \cdot [\phi G_c + \varepsilon \theta_{P_{c:n}} M_P + \theta_{B_{c:n}} M_B + M_{D_c} + \Omega_{dom} \theta_{Z_{c:n}} M_Z] - U_{S_c} + D(S_c) \quad \text{(A9)}$$

Detrital nitrogen [mmolN m^{-3}] equation

$$\frac{\partial D_n}{\partial t} = (1-\beta_n)(1-\phi)Gn + (1-\varepsilon)M_P + \Omega_{D_n} M_Z - G_{D_n} - M_{D_n} - S(D_n) + D(D_n) \quad \text{(A10)}$$

Detrital carbon [mmolC m^{-3}] equation

$$\frac{\partial D_c}{\partial t} = (1-\beta_c)(1-\phi)Gc + (1-\varepsilon)\theta_{P_{c:n}} M_P + \Omega_{D_c} \theta_{Z_{c:n}} M_Z - G_{D_c} - M_{D_c} - S(D_c) + D(D_c) \quad \text{(A11)}$$

Detrital $CaCO_3$ [mmolC m^{-3}] equation

$$\frac{\partial D_h}{\partial t} = \theta_{Ca} \theta_{P_{c:n}} (G_P + M_P) - M_{D_h} - S(D_h) + D(D_h) \quad \text{(A12)}$$

Dissolved inorganic carbon [mmolC m^{-3}] equation

$$\frac{\partial DIC}{\partial t} = -(1+\theta_{Ca})\theta_{P_{c:n}} F_P - E_{doc} + R_B + R_Z + M_{D_h} + \Omega_{DIC} \theta_{Z_{c:n}} M_Z + F_{atm} + D(DIC) \quad \text{(A13)}$$

Alkalinity [mmolC m^{-3}] equation

$$\frac{\partial ALK}{\partial t} = (Q_N - Q_A)F_P - 2\theta_{Ca}\theta_{P_{c:n}} F_P + E_B + E_Z + 2M_{D_h} + \Omega_A M_Z - \nu A + D(ALK) \quad \text{(A14)}$$

CHL [mg m^{-3}] equation

$$\frac{\partial CHL}{\partial t} = (\rho_{chl} C_{mw} \theta_{P_{c:n}})F_P - (G_P + M_P)(CHL/P) - S(CHL) + D(CHL) \quad \text{(A15)}$$

DMSPp [mmolS m^{-3}] equation

$$\frac{\partial DMSPp}{\partial t} = \theta_{P_{s:n}} \frac{\partial P}{\partial t} = \theta_{P_{s:n}} [(1-\gamma_1)F_P - G_P - M_P - S(P) + D(P)] \quad \text{(A16)}$$

DMSPd [mmolS m^{-3}] equation

$$\frac{\partial DMSPd}{\partial t} = \theta_{P_{s:n}} [\gamma_1 F_P + \alpha_1 G_P + M_P] - U_{DMSPd} - U^P_{DMSPd} - fDMSPd + D(DMSPd) \quad \text{(A17)}$$

DMS [mmolS m^{-3}] equation

$$\frac{\partial DMS}{\partial t} = R_{DMS} + E_{DMS} + fDMSPd - U_{DMS} - DMS_{photo} - DMS_{emiss}(*) + D(DMS) \quad \text{(A18)}$$

[50] (*) This term is applied only to the top model cell.

A2. N/C-Cycles Model Terms

[51] Phytoplankton production (F_P)

$$F_P = F^N_P + F^A_P = JQ_N P + JQ_A P = JQP \quad \text{(A19)}$$

$$J = \mu_P R \quad \text{(A20)}$$

$$\mu_P = \mu^{\max}_P e^{(0.063(T - T_{\max}))} \quad \text{(A21)}$$

$$R = \frac{I_z}{I_s} e^{\left(1 - \frac{I_z}{I_s}\right)} \leq 1 \quad \text{(A22)}$$

$$I_z = I_0 e^{-\left(k_w + k_p \bar{P}\right)z} \quad \text{(A23)}$$

$$\bar{P} = \frac{1}{z}\int_0^z P dz \quad \text{(A24)}$$

$$Q = Q_N + Q_A \leq 1 \quad \text{(A25)}$$

$$Q_N = \frac{\frac{N}{k^N_P} e^{(-\psi A)}}{1 + \frac{N}{k^N_P} + \frac{A}{k^A_P}} \quad \text{(A26)}$$

$$Q_A = \frac{\frac{A}{k^A_P}}{1 + \frac{N}{k^N_P} + \frac{A}{k^A_P}} \quad \text{(A27)}$$

Phytoplankton extra-DOC exudation

$$E_{doc} = \gamma_2 \theta_{P_{c:n}} F_P \quad \text{(A28)}$$

Zooplankton grazing on phytoplankton (G_P), bacteria (G_B), detrital nitrogen (G_{Dn}) and detrital carbon (G_{Dc})

$$G_P = \frac{gZp_P P^2}{k_g(p_P P + p_B B + p_D D_n) + p_P P^2 + p_B B^2 + p_D D^2_n} \quad \text{(A29)}$$

$$G_B = \frac{gZp_B B^2}{k_g(p_P P + p_B B + p_D D_n) + p_P P^2 + p_B B^2 + p_D D_n^2} \quad \text{(A30)}$$

$$G_{D_n} = \frac{gZp_D D_n^2}{k_g(p_P P + p_B B + p_D D_n) + p_P P^2 + p_B B^2 + p_D D_n^2} \quad \text{(A31)}$$

$$G_{D_c} = \left(\frac{D_c}{D_n}\right) G_{D_n} \quad \text{(A32)}$$

$$G_n = G_P + G_B + G_{D_n} \quad \text{(A33)}$$

$$G_c = \theta_{P_{c:n}} G_P + \theta_{B_{c:n}} G_B + G_{D_c} \quad \text{(A34)}$$

Zooplankton production (F_Z) and excretion (E_Z)

$$\theta_f^* = \frac{\beta_n \theta_{Z_{c:n}}}{\beta_c \omega_Z} \quad \text{(A35)}$$

$$\theta_f = \frac{(1-\phi)G_c}{(1-\phi)G_n} \quad \text{(A36)}$$

if $\theta_f > \theta_f^*$ (N-limitation):

$$F_Z = \beta_n (1-\phi) G_n \quad \text{(A37)}$$

$$E_Z = 0 \quad \text{(A38)}$$

if $\theta_f < \theta_f^*$ (C-limitation):

$$F_Z = \frac{\beta_c \omega_Z}{\theta_{Z_{c:n}}} (1-\phi) G_c \quad \text{(A39)}$$

$$E_Z = \left(\frac{\beta_n}{\theta_f} - \frac{\beta_n}{\theta_f^*}\right)(1-\phi) G_c \quad \text{(A40)}$$

Zooplankton respiration

$$R_Z = \beta_c (1-\phi) G_c - \theta_{Z_{c:n}} F_Z \quad \text{(A41)}$$

Bacterial uptake of labile DOC (U_{Lc}), labile DON (U_{Ln})

$$U_{L_c} = \mu_B \theta_{B_{c:n}} B \frac{L_c}{k_{Lc} + L_c} \quad \text{(A42)}$$

$$U_{L_n} = \left(\frac{L_n}{L_c}\right) U_{L_c} \quad \text{(A43)}$$

Bacterial maximum potential uptake of ammonium

$$U_A^* = \mu_B B \frac{A}{k_A + A} \quad \text{(A44)}$$

$$\mu_B = \mu_B^{\max}(1 - \phi_{inhib}) \quad \text{(A45)}$$

$$\phi_{inhib} = \phi_{inhib}^{\max} \frac{I_z}{I_{\max}} \quad \text{(A46)}$$

Bacterial production (F_B), ammonium excretion or uptake (E_B) and respiration (R_B)

$$E_B = U_{L_n} - \left(\frac{\omega_B}{\theta_{B_{c:n}}}\right) U_{L_c} \quad \text{(A47)}$$

if $E_B > 0$ (ammonium excretion)
if $E_B < 0$ (ammonium uptake)
if $U_A^* \geq -E_B$ (C-limitation):

$$F_B = U_{L_n} - E_B = \left(\frac{\omega_B}{\theta_{B_{c:n}}}\right) U_{L_c} \quad \text{(A48)}$$

$$R_B = (1 - \omega_B) U_{L_c} \quad \text{(A49)}$$

if $U_A^* < -E_B$ (N-limitation):

$$E_B = -U_A^* \quad \text{(A50)}$$

$$F_B = U_{L_n} - E_B = U_{L_n} + U_A^* \quad \text{(A51)}$$

$$R_B = \left(\frac{1}{\omega_B - 1}\right) \theta_{B_{c:n}} F_B \quad \text{(A52)}$$

Bacterial hydrolysis of semilabile DOC (U_{Sc}) and semilabile DON (U_{Sn})

$$U_{S_c} = \mu_{Sc} \theta_{B_{c:n}} B \frac{S_c}{k_{Sc} + S_c} \quad \text{(A53)}$$

$$U_{S_n} = \left(\frac{S_n}{S_c}\right) U_{S_c} \quad \text{(A54)}$$

Mortality of phytplankton (M_P), zooplankton (M_Z) and bacteria (M_B)

$$M_P = m_P P \quad \text{(A55)}$$

$$M_Z = \frac{m_Z Z^2}{k_Z + Z} \quad \text{(A56)}$$

$$M_B = m_B B \quad \text{(A57)}$$

Breakdown of detrital nitrogen (M_{Dn}), detrital carbon (M_{Dc}) and detrital $CaCO_3$ (M_{Dh})

$$M_{D_n} = m_{D_n} D_n \tag{A58}$$

$$M_{D_c} = m_{D_c} D_c \tag{A59}$$

$$M_{D_h} = m_{D_h} D_h \tag{A60}$$

Chlorophyll-a production

$$\rho_{chl} = \frac{\theta^m_{chl} JQ}{\alpha_{chl} \theta_{chl} I_z} \tag{A61}$$

$$\theta_{chl} = \frac{CHL}{C_{mw} \theta_{P_{c:n}} P} \tag{A62}$$

A3. S-Cycle Model Terms

[52] S:N phytoplankton internal quota

$$\theta_{P_{s:n}} = \theta^{\min}_{P_{s:n}} + \left(\theta^0_{P_{s:n}} - \theta^{\min}_{P_{s:n}}\right) \frac{\min(I_z, I^*)}{I^*} \tag{A63}$$

$$\theta^0_{P_{s:n}} = \theta^{\max}_{P_{s:n}} - \left(\theta^{\max}_{P_{s:n}} - \theta^{\min}_{P_{s:n}}\right) \frac{I_{\max} - I_0}{I_{\max} - I_{\min}} \tag{A64}$$

Phytoplankton DMS exudation

$$E_{DMS} = \gamma_s DMSPp \tag{A65}$$

$$\gamma_s = \gamma^{\max}_s \frac{Iz}{I_{\max}} \frac{\mu_P}{\mu^{\max}_P} \tag{A66}$$

Phytoplankton DMSPd uptake

$$U^P_{DMSPd} = \frac{DMSPd}{A} \alpha_P F^A_P + \frac{DMSPd}{N} \alpha_P F^N_P \tag{A67}$$

Bacterial DMSPd and DMS uptake

$$U_{DMSPd} = \mu_B \theta_{B_{s:c}} \theta_{B_{c:n}} B \frac{DMSPd}{k_{DMSPd} + DMSPd} \tag{A68}$$

$$U_{DMS} = \mu_B \theta_{B_{s:c}} \theta_{B_{c:n}} \alpha_B B \frac{DMS}{k_{DMS} + DMS} \tag{A69}$$

Bacterial sulfur demand

$$U^*_{DMSPd} = \theta_{B_{s:c}} \theta_{B_{c:n}} F_B \tag{A70}$$

Bacterial DMS production
if $U^*_{DMSPd} < U_{DMSPd}$ (no S-limitation):

$$R_{DMS} = \alpha_2 (U_{DMSPd} - U^*_{DMSPd}) \tag{A71}$$

if $U^*_{DMSPd} \geq U_{DMSPd}$ (S-limitation):

$$R_{DMS} = 0 \tag{A72}$$

DMS photolysis

$$DMS_{photo} = k_{photo} DMS \tag{A73}$$

$$k_{photo} = k^{\max}_{photo} \frac{Iz}{I_{\max}} \tag{A74}$$

DMS emission to the atmosphere

$$DMS_{emiss} = k_{emiss} DMS \tag{A75}$$

$$k_{emiss} = \frac{k_v \frac{24}{100}}{\Delta z} \tag{A76}$$

$$k_v = \left(0.24U^2 + 0.061U\right) \left(\frac{Sc}{600}\right)^{(-0.5)} \tag{A77}$$

$$Sc = 2674 - 147.12(SST) + 3.726\left(SST^2\right) - 0.038\left(SST^3\right) \tag{A78}$$

DMS yield

$$DMS_{yield} = \frac{DMS_{prod.}}{DMSP_{cons.}} = \frac{E_{DMS} + R_{DMS} + fDMSPd}{E_{DMS} + U_{DMSPd} + U^P_{DMSPd} + fDMSPd} \tag{A79}$$

A4. Advection (Sinking) and Diffusion Terms

[53] Phytoplankton and Detritus sinking

$$S(X_i) = |\vec{w}_i| \frac{\partial X_i}{\partial z} \tag{A80}$$

for $X_i = P$, D_n, D_c, D_h and CHL. Turbulent diffusion

$$D(X_i) = \frac{\partial}{\partial z} \left(kz \frac{\partial X_i}{\partial z}\right) \tag{A81}$$

for $X_i = P$, Z, B, N, A, L_n, L_c, S_n, S_c, D_n, D_c, D_h, DIC, ALK, CHL, $DMSPp$, $DMSPd$ and DMS.

A5. Turbulent Diffusion and Temperature Profiles

[54]

$$D^* = \frac{D^*_{\max} + D^*_{\min} e^{r\left(D^*_{\min} - D^*_{\max}\right)^{\frac{2(z^* - MLD^*)}{H^*}}}}{1 + e^{r\left(D^*_{\min} - D^*_{\max}\right)^{\frac{2(z^* - MLD^*)}{H^*}}}} \tag{A82}$$

where the asterisk symbol denotes normalized variables (values between 0 and 1):

$$X^* = X/H \tag{A83}$$

$$Y^* = Y/D_{\max} \tag{A84}$$

for $X = z$, MLD, H, and $Y = D$, $D_{\min}$, $D_{\max}$. H is the model vertical domain (200 m) and D can be either diffusion (kz) or sea temperature (st).

A6. Numerical Scheme for Solving the 1-D Model

[55] The general form of the model equations is:

$$\frac{\partial X_i}{\partial t} = J_i - |\vec{w}_i|\frac{\partial X_i}{\partial z} + \frac{\partial}{\partial z}\left(kz\frac{\partial X_i}{\partial z}\right) = f(X_i) \tag{A85}$$

where J_i are the biological source/sink terms for each variable i as defined above, $|\vec{w}_i|\frac{\partial X_i}{\partial z}$ is the vertical sinking (only applies to phytoplankton and detritus), and $\frac{\partial}{\partial z}\left(kz\frac{\partial X_i}{\partial z}\right)$ is the vertical turbulent diffusion. The numerical scheme is implemented using a finite difference approximation. At each time step and for each vertical grid point j, all three terms are calculated independently to obtain $f(X_i)$. The sinking term is calculated using a first-order upwind discretization:

$$\frac{\partial X_i^j}{\partial z} = \frac{X_i^{j-1} - X_i^j}{\Delta z} \tag{A86}$$

while the diffusion term is calculated using a second-order centered discretization:

$$\frac{\partial}{\partial z}\left(kz\frac{\partial X_i}{\partial z}\right) = \frac{kz^{j+1/2}\left(X_i^{j+1} - X_i^j\right) - kz^{j-1/2}\left(X_i^j - X_i^{j-1}\right)}{(\Delta z)^2} \tag{A87}$$

where $kz^{j+1/2} \equiv kz(z_{j+j/2})$. Finally, for each vertical grid point we then advance the solution in time from X_i^t to X_i^{t+1} using a forward Euler method [*Press et al.*, 1992]:

$$X_i^{t+1} = X_i^t + f\left(X_i^t\right)\Delta t \tag{A88}$$

[56] **Acknowledgments.** Our special thanks to E. E. Popova for her kindly assistance and advice during the computer coding of the model. The authors would also like to thank the two reviewers (Scott Elliott and Dierdre Toole) for their thorough and very constructive review. This work was supported by the Spanish Ministry of Education and Science (MEC) through the projects AMIGOS (contract REN2001-3462/CLI to R.S.) and MIMOSA (contract CTM2005-06513 to R.S.), and a Ph.D. studentship (to S.M.V.). T. R. Anderson is funded by the Natural Environment Research Council (NERC, U.K.). This work is a contribution to the objectives of the SOLAS project and the Eur-Oceans Network of Excellence of the 6th Framework Program of the EU.

References

Albrecht, B. A. (1989), Aerosols, cloud microphysics, and fractional cloudiness, *Science*, *245*(4923), 1227–1230.

Anderson, T. R. (1992), Modeling the influence of food C:N ratio, and respiration on growth and nitrogen excretion in marine zooplankton and bacteria, *J. Plankton Res.*, *14*, 1645–1671.

Anderson, T. R., and D. O. Hessen (1995), Carbon or nitrogen limitation of marine copepods?, *J. Plankton Res.*, *17*, 317–331.

Anderson, T. R., and P. J. le B. Williams (1998), Modelling the seasonal cycle of dissolved organic carbon at Station E1 in the English Channel, *Estuarine Coastal Shelf Sci.*, *46*, 93–109.

Anderson, T. R., and P. Pondaven (2003), Non-redfield carbon and nitrogen cycling in the Sargasso Sea: pelagic imbalances and export flux, *Deep Sea Res., Part I*, *50*, 573–591.

Andreae, M. O., and P. J. Crutzen (1997), Atmospheric aerosols: biogeochemical sources and role in the atmospheric chemistry, *Science*, *276*, 1052–1058.

Archer, S. D., F. J. Gilbert, P. D. Nightingale, M. V. Zubkov, A. H. Taylor, G. C. Smith, and P. H. Burkill (2002), Transformation of dimethylsulphoniopropionate to dimethyl sulphide during summer in the North Sea with an examination of keyprocesses via a modelling approach, *Deep Sea Res., Part II*, *49*, 3067–3101.

Bailey, K. E., D. A. Toole, B. Blomquist, R. G. Najjar, B. Huebert, D. J. Kieber, R. P. Kiene, P. Matrai, G. R. Westby, and D. A. del Valle (2008), Estimation of dimethylsulfide production in Sargasso Sea Eddies, *Deep Sea Res.*, in press.

Baretta, J. W., W. Ebenhöh, and P. Ruardij (1995), The European Regional Seas Ecosystem Model, a complex marine ecosystem model, *Neth. J. Sea Res.*, *33*, 233–246.

Bates, T. S., B. K. Lamb, A. Guenther, J. Dignon, and R. E. Stoiber (1992), Sulfur emissions to the atmosphere from natural sources, *J. Atmos. Chem.*, *14*, 315–337.

Bates, T. S., R. P. Kiene, G. V. Wolfe, P. A. Matrai, F. P. Chavez, K. R. Buck, B. W. Blomquist, and R. L. Cuhel (1994), The cycling of sulfur in surface seawater of the Northeast Pacific, *J. Geophys. Res.*, *99*, 7835–7843.

Brimblecombe, P., and D. Shooter (1986), Photo-oxidation of dimethylsulfide in aqueous solution, *Mar. Chem.*, *19*, 343–353.

Broecker, W. S., and T. H. Peng (1982), *Tracers in the Sea*, 690 pp., Lamont-Doherty Geol. Obs., Columbia Univ., Palisades, New York.

Brugger, A., D. Slezak, I. Obernosterer, and G. J. Herndl (1998), Photolysis of dimethylsulfide in the northern Adriatic Sea: dependence on substrate concentration, irradiance and DOC concentration, *Mar. Chem.*, *59*, 321–331.

Bucciarelli, E., and W. G. Sunda (2003), Influence of CO_2, nitrate, phosphate, and silicate limitation on intracellular dimethylsulfoniopropionate in batch cultures of the coastal diatom Thalassiosira pseudonana, *Limnol. Oceanogr.*, *48*(6), 2256–2265.

Charlson, R. J., J. E. Lovelock, M. O. Andreae, and S. G. Warren (1987), Oceanic phytoplankton, atmospheric sulfur, cloud albedo and climate, *Nature*, *326*, 655–661.

Chu, S., S. Elliott, M. Maltrud, J. Rodríguez, and D. J. Erickson (2004), Ecodynamic and eddy admitting simulations of dimethyl sulfide distributions in a global ocean biogeochemistry-circulation model, *Earth Interactions*, *8*, 1–25.

Cropp, R. A. (2002), A biogeochemical modelling analysis of the potential for marine ecosystems to regulate climate by the production of dimethylsulfide, Ph.D. thesis.

Cropp, R. A., J. Norbury, A. J. Gabric, and R. D. Braddock (2004), Modeling dimethylsulphide production in the upper ocean, *Global Biogeochem. Cycles*, *18*, GB3005, doi:10.1029/2003GB002126.

Dacey, J. W. H., F. A. Howse, A. F. Michaels, and S. G. Wakeham (1998), Temporal variability of dimethylsulfide and dimethylsulfoniopropionate in the Sargasso Sea, *Deep Sea Res., Part I*, *45*, 2085–2104.

del Valle, D. A., D. J. Kieber, and R. P. Kiene (2007), Depth-dependent fate of biologically-consumed dimethylsulfide in the Sargasso Sea, *Mar. Chem.*, *103*, 197–208.

Denman, K. L., and M. A. Peña (1999), A coupled 1-D biological/physical model of the northeast subarctic Pacific Ocean with iron limitation, *Deep Sea Res., Part II*, *46*, 2877–2908.

DuRand, M. D., R. J. Olson, and S. W. Chisholm (2001), Phytoplankton population dynamics at the Bermuda Atlantic Time-series station in the Sargasso Sea, *Deep Sea Res., Part II*, *41*, 1983–2003.

Eigenheer, A., W. Kuhn, and G. Radach (1996), On the sensitivity of ecosystem box model simulations on mixed-layer depth estimates, *Deep Sea Res., Part I*, *43*, 1011–1027.

Eppley, R. W. (1972), Temperature and phytoplankton growth in the sea, *Fish. Bull.*, *70*(4), 1063–1085.

Gabric, A., N. Murray, L. Stone, and M. Kohl (1993), Modeling the production of dimethylsulfide during a phytoplankton bloom, *J. Geophys. Res.*, *98*, 22,805–22,816.

Gabric, A. J., B. Qu, P. Matrai, and A. C. Hirst (2005), The simulated response of dimethylsulfide production in the Arctic Ocean to global warming, *Tellus, Ser. B*, *57*, 391–403.

Geider, R. J., H. MacIntyre, and T. M. Kana (1997), Dynamic model of phytoplankton growth and acclimation: responses of the balanced growth

rate and the chlorophyll a: carbon ratio to light, nutrient-limitation and temperature, *Mar. Ecol. Prog. Ser.*, *148*, 187–200.
Goericke, R. (1998), Response of phytoplankton community structure and taxon-specific growth rates to seasonally varying physical forcing in the Sargasso Sea of Bermuda, *Limnol. Oceanogr.*, *43*(5), 921–935.
González, J. M., R. P. Kiene, and M. A. Moran (1999), Transformation of sulfur compounds by an abundant lineage of marine bacteria in the α-subclass of the class *Proteobacteria*, *Aquat. Environ. Microbiol.*, *65*(9), 3810–3819.
Groene, T. (1995), Biogenic production and consumption of dimethylsulfide (DMS) and dimethylsulfoniopropionate (DMSP) in the marine epipelagic zone: a review, *J. Mar. Syst.*, *6*, 191–209.
Gundersen, K., M. Heldal, S. Norland, D. A. Purdie, and A. H. Knap (2002), Elemental C, N, and P cell content of individual bacteria collected at the Bermuda Atlantic Time-Series Study (BATS) site, *Limnol. Oceanogr.*, *47*(5), 1525–1530.
Herndl, G. J., G. Müller-Niklas, and J. Frick (1993), Major role of ultraviolet-B in controlling bacterioplankton growth in the surface layer of the ocean, *Nature*, *361*, 717–719, doi:10.1038/361717a0.
Jodwalis, C. M., R. L. Benner, and D. L. Eslinger (2000), Modeling of dimethyl sulfide ocean mixing, biological production, and sea-to-air flux for high latitudes, *J. Geophys. Res.*, *105*(D11), 14,387–14,399.
Kaufman, Y. J., D. Tanre, and O. Boucher (2002), A satellite view of aerosols in the climate system, *Nature*, *419*(6903), 215–223.
Keller, M. D., and W. Korjeff-Bellows (1996), Physiological aspects of the production of dimethylsulfoniopropionate (DMSP) by marine phytoplankton, in *Biological and Environmental Chemistry of DMSP and Related Sulfonium Compounds*, edited by R. P. Kiene, P. T. Visscher, M. D. Keller, and G. O. Kirst, pp.131–142, Plenum, New York.
Keller, M. D., W. K. Bellows, and R. R. L. Guillard (1989), Dimethylsulfide production in marine phytoplankton, in *Biogenic Sulfur in the Environment*, *Am. Chem. Soc. Symp. Ser.*, vol. 393, edited by E. S. Saltzman and W. J. Cooper, pp.167–182, Washington, D. C.
Kettle, A. J., and M. O. Andreae (2000), Flux of dimethylsulfide from the oceans: A comparison of updated data set and flux models, *J. Geophys. Res.*, *105*(D22), 26,793–26,808.
Kieber, D. J., J. Jiao, R. P. Kiene, and T. S. Bates (1996), Impact of dimethylsulfide photochemistry on methyl sulfur cycling in the equatorial Pacific Ocean, *J. Geophys. Res.*, *101*(C2), 3715–3722.
Kiene, R. P. (1992), Dynamics of dimethylsulfide and dimethylsulfoniopropionate in oceanic water samples, *Mar. Chem.*, *37*, 29–52.
Kiene, R. P. (1993), Microbial sources and sinks for methylated sulfur compounds in the marine environment, in *Microbial Growth on C1 Compounds*, vol. 7, edited by D. P. Kelly and J. C. Murrell, pp. 15–33, Intercept, London, UK.
Kiene, R. P. (1996), Production of methanethiol from dimethylsulfoniopropionate in marine surface waters, *Mar. Chem.*, *54*, 69–83.
Kiene, R. P., and T. S. Bates (1990), Biological removal of dimethylsulfide from sea water, *Nature*, *345*, 702–705.
Kiene, R. P., and L. J. Linn (2000), The fate of dissolved dimethylsulfoniopropionate (DMSP) in seawater: Tracer studies using 35S-DMSP, *Geochim. Cosmochim. Acta*, *64*(16), 2797–2810.
Kiene, R. P., and D. Slezak (2006), Low dissolved DMSP concentrations in seawater revealed by small-volume gravity filtration and dialysis sampling, *Limnol. Oceanogr. Methods*, *4*, 80–95.
Kiene, R. P., L. J. Linn, J. González, M. A. Moran, and J. A. Bruton (1999), Dimethylsulfoniopropionate and methanethiol are important precursors of methionine and protein-sulfur in marine bacterioplankton, *Aquat. Environ. Microbiol.*, *65*(10), 4549–4558.
Kiene, R. P., L. J. Linn, and J. A. Bruton (2000), New and important roles for DMSP in marine microbial communities, *J. Sea. Res.*, *43*, 209–224.
Laroche, D., A. F. Vézina, M. Levasseur, M. Gosselin, J. Stefels, M. D. Keller, P. A. Matrai, and R. L. J. Kwint (1999), DMSP synthesis and exudation in phytoplankton: a modeling aproach, *Mar. Ecol. Prog. Ser.*, *180*, 37–49.
Lawrence, M. (1993), An empirical analysis of the strength of the phytoplankton-dimethylsulfide-cloud-climate feedback cycle, *J. Geophys. Res.*, *98*, 20,663–20,763.
Le Clainche, Y., M. Levasseur, A. Vézina, J. W. H. Dacey, and F. J. Saucier (2004), Behaviour of the ocean DMS (P) pools in the Sargasso Sea viewed in a coupled physical-biogeochemical ocean model, *Can. J. Fish. Aquat. Sci.*, *61*, 788–803.
Ledyard, K. M., and J. W. H. Dacey (1996), Microbial cycling of DMSP and DMS in coastal and oligotrophic seawater, *Limnol. Oceanogr.*, *41*, 33–40.
Lefevre, M., A. Vézina, M. Levasseur, and J. W. H. Dacey (2002), A model of dimethylsulfide dynamics for the subtropical North Atlantic, *Deep Sea Res., Part I*, *49*, 2221–2239.
Levasseur, M., S. Michaud, J. Egge, G. Cantin, J. C. Nejstgaard, R. Sanders, E. Fernández, P. T. Solberg, B. Heimdal, and M. Gosselin (1996), Production of DMSP and DMS during a mesocosm study of an Emiliania huxleyi bloom: Influence of bacteria and Calanus finmarchicus grazing, *Mar. Biol.*, *126*(4), 609–618.
Levasseur, M., M. Scarratt, S. Roy, D. Laroche, S. Michaud, G. Cantin, M. Gosselin, and A. Vézina (2004), Vertically resolved cycling of dimethylsulfoniopropionate (DMSP) and dimethylsulfide (DMS) in the Northwest Atlantic in spring, *Can. J. Fish. Aquat. Sci.*, *61*, 744–757.
Levitus (1982), Climatological atlas of the world, *NOAA Prof. Pap., 30*.
Malmstrom, R. R., R. P. Kiene, and D. L. Kirchman (2004), Identification and enumeration of bacteria assimilating dimethylsulfoniopropionate (DMSP) in the North Atlantic and Gulf of Mexico, *Limnol. Oceanogr.*, *49*(2), 597–606.
Moloney, C. L., M. O. Bergh, J. G. Field, and R. C. Newell (1986), The effect of sedimentation and microbial nitrogen regeneration in a plankton community: a simulation investigation, *J. Plankton Res.*, *8*, 426–445.
Nightingale, P. D., G. Malin, C. S. Law, A. J. Watson, P. S. Liss, M. I. Liddicoat, J. Boutin, and R. C. Upstill-Goddard (2000), In situ evaluation of air-sea gas exchange parameterizations using novel conservative and volatile tracers, *Global Biogeochem. Cycles*, *14*, 373–387.
Niki, T., M. Kunugi, and A. Otsuki (2000), DMSP-lyase activity in five marine phytoplankton species: its potential importance in DMS production, *Mar. Biol.*, *136*, 759–764.
Popova, E. E., C. J. Lozano, M. A. Srokosz, M. J. R. Fasham, P. J. Haley, and A. R. Robinson (2002), Coupled 3D physical and biological modelling of the mesoscale variability observed in northeast Atlantic in spring 1997: biological processes, *Deep Sea Res., Part I*, *49*, 1741–1768.
Press, W. H., B. P. Flannery, S. A. Teukolsky, and W. T. Vetterling (1992), *Numerical Recipes in FORTRAN: The Art of Scientific Computing*, 2nd ed., p.710, Cambridge Univ. Press, Cambridge, UK.
Simó, R. (2001), Production of atmospheric sulfur by oceanic plankton: biogeochemical, ecological and evolutionary links, *Trends Ecol. Evol.*, *16*(6), 287–294.
Simó, R. (2004), From cells to globe: approaching the dynamics of DMS(P) in the ocean at multiple scales, *Can. J. Fish. Aquat. Sci.*, *61*, 673–684.
Simó, R., and C. Pedrós-Alió (1999), Role of vertical mixing in controlling the oceanic production of dimethyl sulphide, *Nature*, *402*, 396–399.
Simó, R., C. Pedrós-Alió, G. Malin, and J. O. Grimalt (2000), Biological turnover of DMS, DMSP and DMSO in contrasting open-sea waters, *Mar. Ecol. Prog. Ser.*, *203*, 1–11.
Slezak, D., and G. J. Herndl (2003), Effects of ultraviolet and visible radiation on the cellular concentrations of dimethylsulfoniopropionate (DMSP) in *Emiliania huxleyi* (strain L), *Mar. Ecol. Prog. Ser.*, *246*, 61–71.
Slezak, D., A. Brugger, and G. J. Herndl (2001), Impact of solar radiation on the biological removal of dimethylsulfoniopropionate and dimethylsulfide in marine surface waters, *Aquat. Microbial Ecol.*, *25*, 87–97.
Spitz, Y. H., J. R. Moisan, and M. R. Abbott (2001), Configuring an ecosystem model using data from the Bermuda Atlantic Time Series (BATS), *Deep Sea Res., Part II*, *48*, 1733–1768.
Stefels, J. (2000), Physiological aspects of the production and conversion of DMSP in marine algae and higher plants, *J. Sea Res.*, *43*, 183–197.
Stefels, J., and M. A. van Leeuwe (1998), Effects of iron and light stress on the biochemical composition of antarctic *Phaeocystis* sp. (Prymnesiophyceae): I. Intracellular DMSP concentrations, *J. Phycol.*, *34*, 486–495.
Steinberg, D. K., C. A. Carlson, N. R. Bates, R. J. Johnson, A. F. Michaels, and A. H. Knap (2001), Overview of the US JGOFS Bermuda Atlantic Time-series Study (BATS): a decade-scale look at ocean biology and biogeochemistry, *Deep Sea Res., Part II*, *48*, 1405–1447.
Steinke, M., G. Malin, and P. S. Liss (2002a), Trophic interactions in the sea: An ecological role for climate relevant volatiles?, *J. Phycol.*, *38*, 630–638.
Steinke, M., G. Malin, S. D. Archer, P. H. Burkill, and P. S. Liss (2002b), DMS production in a coccolithophorid bloom: evidence for the importance of dinoflagellate DMSP lyases, *Aquat. Microbial Ecol.*, *26*, 259–270.
Sunda, W., D. J. Kleber, R. P. Kiene, and S. Huntsman (2002), An antioxidant function for DMSP and DMS in marine algae, *Nature*, *418*, 317–320.
Toole, D. A., and D. A. Siegel (2004), Ligth-driven cycling of dimethylsulfide (DMS) in the Sargasso Sea: Closing the loop, *Geophys. Res. Lett.*, *31*, L09308, doi:10.1029/2004GL019581.
Toole, D. A., D. J. Kieber, R. P. Kiene, D. A. Siegel, and N. B. Nelson (2003), Photolysis and the dimethylsulfide (DMS) summer paradox in the Sargasso Sea, *Limnol. Oceanogr.*, *48*, 1088–1100.
Toole, D. A., D. Slezak, R. P. Kiene, D. J. Kieber, and D. A. Siegel (2006), Effects of solar radiation on dimethylsulfide cycling in the western Atlantic Ocean, *Deep Sea Res., Part I*, *53*, 136–153.
Twomey, S. (1974), Pollution and planetary albedo, *Atmos. Environ.*, *8*, 1251–1256.
Uher, G., G. Schebeske, R. G. Barlow, D. G. Cummings, R. F. C. Mantoura, S. R. Rapsomanikis, and M. O. Andreae (2000), Distribution and air-sea

gas exchange of dimethyl sulphide at the European western continental margin, *Mar. Chem.*, *69*, 277–300.

Vairavamurthy, A., M. O. Andreae, and R. L. Iverson (1985), Biosynthesis of dimethylsulfide and dimethylpropiothetin by Hymenomonas carterae in relation to sulfur source and salinity variations, *Limnol. Oceanogr.*, *30*(1), 59–70.

Vallina, S. M., and R. Simó (2007), Strong relationship between DMS and the solar radiation dose over the global surface ocean, *Science*, *315*, 506–508.

Vallina, S. M., R. Simó, and S. Gassó (2006), What controls CCN seasonality in the Southern Ocean? A statistical analysis based on satellite-derived chlorophyll and CCN and model-estimated OH radical and rainfall, *Global Biogeochem. Cycles*, *20*, GB1014, doi:10.1029/2005GB002597.

Vallina, S. M., R. Simó, S. Gassó, C. de Boyer-Montégut, E. del Río, E. Jurado, and J. Dachs (2007), Analysis of a potential "Solar Radiation Dose - DMS - CCN" link from globally mapped seasonal correlations, *Global Biogeochem. Cycles*, *21*, GB2004, doi:10.1029/2006GB002787.

van den Berg, A., S. Turner, F. van Duyl, and P. Ruardij (1996), Model structure and analysis of dimethylsulphide (DMS) production in the southern North Sea, considering phytoplankton dimethylsulphoniopropionate- (DMSP) lyase and eutrophication effects, *Mar. Ecol. Prog. Ser.*, *145*, 233–244.

Vézina, A. F. (2004), Ecosystem modelling of the cycling of marine dimethylsulfide: a review of current approaches and of the potential for extrapolation to global scales, *Can. J. Fish. Aquat. Sci.*, *61*, 845–856.

Vila, M., R. Simó, R. P. Kiene, J. Pinhassi, J. M. González, M. A. Moran, and C. Pedrós-Alió (2004), Use of microautoradiography combined with fluorescence in situ hybridization to determine dimethylsulfoniopropionate incorporation by marine bacterioplankton taxa, *Aquat. Environ. Microbiol.*, *70*(8), 4648–4657.

Vila-Costa, M. (2006), Seasonality of DMSP contribution to S and C fluxes through phytoplankton and bacterioplankton in a NW Mediterranean coastal site, in *Major Players in the Biogeochemical Cycling of Dimethylated Sulfur Compounds in Seawater*, Ph.D. thesis, chap. 4, Univ. Politecnica de Catalunya. (Available at http://www.cmima.csic.es./pub/gasol/tesi_laura/MASTER_Tesi_Sense_Linies.pdf)

Vila-Costa, M., D. A. del Valle, J. M. González, D. Slezak, R. P. Kiene, O. Sánchez, and R. Simó (2006a), Phylogenetic identification and metabolism of marine dimethylsulfide-consuming bacteria, *Environ. Microbiol.*, *8*(12), 2189–2200, doi:10.1111/j.1462-2920.2006.01102.x.

Vila-Costa, M., R. Simó, J. M. Gasol, B. Harada, D. Slezak, and R. P. Kiene (2006b), Dimethylsulfoniopropionate (DMSP) uptake by marine phytoplankton, *Science*, *314*, 652–654.

Vila-Costa, M., R. P. Kiene, C. Alonso, J. Pertnhaler, J. Phinassi, and R. Simó (2007), Seasonal variation of DMSP-assimilating bacteria in the coastal NW Mediterranean, *Environ. Microbiol.*, *9*, 2451–2463.

Vila-Costa, M., R. P. Kiene, and R. Simó (2008), Seasonal variability of the dynamics of dimethylated sulfur compounds in a NW Mediterranean site, *Limnol. Oceanogr.*, in press.

Walsh, J., D. A. Dieterle, and J. Lenes (2001), A numerical analysis of carbon dynamics of the Southern Ocean phytoplankton community: The roles of light and grazing in effecting both sequestration of atmospheric CO_2 and food availability to larval krill, *Deep Sea Res., Part I*, *48*, 1–48.

Wolfe, G. V., M. Levasseur, G. Cantin, and S. Michaud (1999), Microbial consumption and production of dimethylsulfide (DMS) in the Labrador Sea, *Aquat. Microbial Ecol.*, *18*, 197–205.

Wolfe, G. V., S. L. Strom, J. L. Holmes, T. Radzio, and M. B. Olson (2002), Dimethylsulfoniopropionate cleavage by marine phytoplankton in response to mechanical, chemical, or dark stress, *J. Phycol.*, *38*, 948–960.

Yoch, D. C. (2002), Dimethylsulfoniopropionate: Its sources, role in the marine food web, and biological degradation to dimethylsulfide, *Aquat. Environ. Microbiol.*, *68*(12), 5804–5815.

Yoch, D. C., J. H. Ansede, and K. S. Rabinowitz (1997), Evidence for intracellular and extracellular dimethylsulfoniopropionate (DMSP) lyases and DMSP uptake sites in two species of marine bacteria, *Aquat. Environ. Microbiol.*, *63*(8), 3182–3188.

Zubkov, M., L. J. Linn, R. Amann, and R. P. Kiene (2004), Temporal patterns of biological dimethylsulfide (DMS) consumption during laboratory-induced phytoplankton bloom cycles, *Mar. Ecol. Prog. Ser.*, *271*, 77–86.

Zubkov, M. V., B. M. Fuchs, S. D. Archer, R. P. Kiene, R. Amann, and P. Burkill (2001), Linking the composition of bacterioplankton to rapid turnover of dissolved dimethylsulphoniopropionate in an alglal bloom in the North Sea, *Environ. Microbiol.*, *3*(5), 304–311.

Zubkov, M. V., B. M. Fuchs, S. D. Archer, R. P. Kiene, R. Amann, and P. H. Burkill (2002), Rapid turnover of dissolved DMS and DMSP by defined bacterioplankton communities in the stratified euphotic zone of the North Sea, *Deep Sea Res., Part II*, *49*, 3017–3038.

T. R. Anderson, National Oceanography Center (NOC), Southampton SO14 3ZH, UK.

R. Cropp and A. Gabric, Faculty of Environmental Sciences, Griffith University, Nathan, Qld 4111, Australia.

J. M. Pacheco, Departamento de Matemáticas, Facultad de Ciencias del Mar, Universidad de Las Palmas de Gran Canaria (FCM - ULPGC), 35017 Islas Canarias, Spain.

R. Simó, Institut de Ciències del Mar de Barcelona (ICM - CSIC), Passeig Marítim de la Barceloneta, 37-49, 08003 Barcelona, Spain.

S. M. Vallina, School of Environmental Sciences, University of East Anglia (ENV - UEA), Norwich NR4 7TJ, UK. (sergio.vallina@uea.ac.uk)